Silicon (2022) 14:5751–5782
https://doi.org/10.1007/s12633-021-01340-9

REVIEW PAPER

Mechanical and Tribological Properties of 3D printed Al-Si alloys and composites: a Review

Bheemavarapu Subba Rao [1,2] · Thella Babu Rao [1]

Received: 17 January 2021 / Accepted: 18 August 2021 / Published online: 7 September 2021

Abstract
Aluminum alloys were used in engineering applications, such as aircraft, aerospace, automobiles, and various other fields due to being light-weight, have relatively high strength, retain good ductility at sub-zero temperatures, have high corrosion resistance, and are non-toxic. Three-dimensional printing was used for the fabrication of aluminum alloys and aluminum metal matrix composites with high precision, shorter lead time, cost-effectiveness compared to traditional manufacturing. In the 3D printing process, Al-Si alloys and composites were produced by using powder-based manufacturing techniques, such as Selective Laser Melting (SLM), Laser Powder Bed Fusion (LPBF), and Direct Metal Laser Sintering (DMLS) due to their higher laser absorption. The mechanical properties of built parts were improved compared to the traditional manufacturing process and some drawbacks in surface finishing, dimensional accuracy. The mechanical and tribological properties of 3D printing Al-Si alloys were dependent upon process and process parameters. Pre and post-processing methods were used to improve the mechanical and tribological properties. In this paper, an attempt has been made to review the mechanical and tribological properties of 3D printing Al-Si alloys and their composites in various additive manufacturing processes with varying process parameters and to review the effect of pre and post-processing methods on mechanical and tribological properties of 3D printing Al-Si alloys and their composites before and after pre and post-processing methods. The mechanical properties of Al-Si alloys produced in 3D printing methods were more compared to the conventional manufacturing methods. The ductility of the 3D printed Al-Si alloys were improved in heat treatment methods, such as hot isostatic pressing, annealing, and solution heat treatment methods. The 3D printing methods were successfully used for manufacturing Al-Si metal matrix components. The wear resistance of the 3D printed Al-Si metal matrix components were more compared to the conventional manufacturing Al-Si metal matrix components.

Keywords 3D printing · Al-Si alloys · Al-Si composites · process parameters · pre and post-processing methods · Mechanical Properties · Tribological properties

1 Introduction

Three-dimensional (3D) printing is also called additive manufacturing (AM), described first in 1986 by Charles [1]. It is defined as the process of adding material layer-by-layer with a layer thickness as small as 20μm to make components from 3D CAD models [2–4].The AM process accorded with several advantages like flexibility in design, higher productivity, less wastage in material and energy over the conventional way of manufacturing the industrial components [5]. The developments in additive manufacturing processes during the last three decades invited the manufacturing of a widely range of functional and operational industrial parts [6–9] made of plastics, ceramics, and metals with in competitive costs and times [10–13]. Different type of materials used in additive manufacturing process for making the functional parts, are stainless steels [14,15], titanium [16,17], nickel [18,-19],copper [20,21],gold [22], aluminum alloys [23–25], metal matrix composites [26,27] and ceramic materials [26]. The use of AM process is also gained attraction for manufacturing of complex rapid prototyping tools with design flexibility [28].

✉ Bheemavarapu Subba Rao
subbu4engg@gmail.com

Thella Babu Rao
thellababurao@nitandhra.ac.in

[1] Department of Mechanical Engineering, National Institute of Technology Andhra Pradesh, Tadepalligudem, West Godavari Dist., Andhra Pradesh 534101, India

[2] D.A. Govt. Polytechnic, Ongole, Andhra Pradesh, India

Small batch sizes are produced in AM at a reasonable cost [29]. The time gap between design and manufacturing is reduced by reducing the wastages and replacing the manufacturing process with a single process in AM [30, 31]. Parts produced in AM are used in different applications, in medical such as dental prostheses, orthopedic implants [32], in the aerospace industry such as lightweight scaffold implants structures [33], in the automotive and power sector [34–35]. The limitations in metal AM are the size of the part which intern depends upon the size of the machine chamber, higher machine cost, poorer surface finish, product anisotropy, and cost of the powders [36–37]. In the industry 4.0 revolution, AM is one of the leading sectors [38–39].

Aluminum alloys and their composites are used for various engineering applications in aircraft, aerospace, automobiles, electronics, and railway industries. The attractive characteristics of these materials for such applications are lightweight, high strength, high stiffness, and high load to weight ratio, tremendous wear resistance, corrosion resistance, excellent electrical and thermal conductivity, and low thermal expansion coefficient [40–44]. Depending upon the alloy, they have a melting point temperature range between 482°C and 660°C [45]. In traditional manufacturing, aluminum and its alloys are produced by using casting, extrusion, and forging processes. The disadvantages in conventional manufacturing are the delays in the production process, high cost, formation of thin-walled and irregular shapes during the production of complex geometry structures [46]. AM in the present industrial sectors is gaining more attention to fabricating aluminum alloy-based functional components as a new manufacturing technology. Initially, the AM process is used to produce the prototypes, and later, it is being used to create highly complex parts [47]. Through continues development and research, 3D printing techniques switched from “rapid prototyping” into “rapid manufacturing” [48]. The recent technological advancements emerging for metal parts manufacturing are Selective Laser Melting (SLM) [49], Laser Powder Bed Fusion (LPBF) [50], and Direct Metal Laser Sintering (DMLS) [51].

As with the conventional manufacturing process, the mechanical and tribological properties of AM components also depend upon their processing parameters. The internal stress of the LPBF Ti-6Al-4V alloy is lower at higher laser power [52]. The laser power affects the porosity of the built parts. The porosity of the SLM 15-5PH stainless steel decreases with decreasing the laser power [53]. The porosity of the LPBF 316L stainless increases with reducing the laser power [54]. The tensile strength of the additive manufacturing parts increases with increasing the laser scanning velocity [55]. The porousness of the SLM 15-5PH stainless steel decreases with increasing the laser scanning velocity [54]. The laser scanning velocity affects the mechanical features of the SLM 316L stainless steel [56]. Higher relative density of the SLM 316L stainless steel and better mechanical properties were obtained at higher laser scanning speed [57]. The hatch spacing affects the ultimate tensile of the 3D printed parts. The maximum tensile strength of SLM Ti–6Al–4V alloy decreases with increasing the hatch spacing [58]. The tensile strength of the SLM 316L stainless steel increases with increasing the sample thickness from 1mm to 3mm [59]. Gan et al. [60] examined the effect of SLM 18Ni300 steel extracting parameters on hardness, the higher hardness of the built samples obtained at a laser power of 150~200W, a laser scanning velocity 600mm/s, and hatch spacing of 0.105mm. The post-heat treatment methods are used to enhance the mechanical features of 3D printed samples. The mechanical characteristics of the SLM Zr-modified AA6061 alloy are increased after the T6 heat treatment [61]. The mechanical features of the SLM Al-Cu alloy components improved after aging heat treatment [62]. The mechanical characteristics of the SLM AlSi10Mg alloy components were improved after heat treatment at 175°C for 6h [63]. The additive manufacturing methods are used to fabricate the aluminum-based metal matrix composites, and the mechanical properties of aluminum alloys are improved by reinforcement particles [64–66].

2 3D printing methods

According to ASTM F42 standards, 3D printing methods are classified as (i) material extrusion,(ii) vat polymerization,(iii) binder jetting,(iv) material jetting, (v) powder bed fusion,(vi)sheet lamination, and (vii) direct energy deposition [67]. These technologies are evolved for manufacturing different parts made of polymers, photopolymers, ceramic, and metallics. Binder jetting, material extrusion and powder bed fusion are used for polymers, while material jetting and vat polymerization are used for photopolymers. Binder jetting, powder bed fusion, sheet lamination, and vat polymerization are used for ceramics, and sheet metal lamination is used for metallic sheets. Binder jetting, powder bed fusion and direct energy deposition [68] are adopted for metal AM. The inherent physical properties with aluminum alloys, such as high laser reflectivity, formation of oxide film, thermal expansion, and high thermal conductivity, restricted the application of 3D printing methods for widespread manufacturing of industrial components compared with the steel, titanium (Ti), nickel (Ni) based alloys. Due to the higher laser absorption property with the Al-Si alloys made them easy to process using laser-based AM approaches compared with their allied alloys. Hence, powder bed fusion and direct energy deposition methods are more pronounced AM processes for manufacturing Al-Si alloy components. Electron beam, laser energy, and welding arc sources are used to fuse the feedstock material in the direct energy deposition method. The wire is used as a feedstock material in electron beam and welding arc, while powder is the feedstock material in the laser energy source [69–72].

Direct energy deposition is referred to as Direct Metal Deposition (DMD), Laser Metal Deposition (LMD), Laser Engineered Net Shaping (LENS), or Electron Beam Melting (EBM) [73]. DMD and LENS methods are used for additive manufacturing of Al-Si alloys [74–77]. Compared to the Powder Bed Fusion process, the porosity of built parts is higher, and relative density is less in the DED method [77]. Coarse microstructures are observed in the DED due to temperature cycle history, and the internal cooling rate is less during the process, and layer thickness is higher compared to the powder bed fusion process [74,75]. Powder Bed Fusion is referred to as Laser Powder Bed Fusion, Selective Laser Melting, and Direct Metal Laser Sintering, but the principle of operation is the same in all cases [73]. Compared to the Direct Energy Deposition method, the Powder Bed Fusion methods are widely used to manufacture Al-Si alloys. In the Powder Bed Fusion method, Selective Laser Melting (SLM), Laser Powder Bed Fusion (LPBF), Direct Metal Laser Sintering (DMLS) technologies are widely used to produce Al-Si components [49–51].

2.1 Selective Laser Melting

SLM is one type of powder-based three-dimensional printing technique used for manufacturing metal parts since the 1980s [78]. It is used to produce parts with complex shapes [79]. In SLM, the final part is made by laser fusion of powder material based on the CAD input model [80–82]. The working principle of the SLM process is shown in Fig. 1. SLM is an eminent metal 3D printing process. It is also known as DMLS [83], Laser Metal Fusion (LMF) [84], and Laser Beam Melting (LBM) [85], depending upon the manufacturers of the machine. Nowadays, industries need design freedom, manufacturing flexibility, and the depletion of cost and time for complex parts [86–88]. The mechanical strength and surface quality of functional parts produced in the SLM process are higher than the conventional parts [89,90]. The mechanical properties of the SLM components are superior to the traditional casting and powder metallurgy processes due to the rapid cooling [91–93]. Due to the fast solidification and high freezing rates, very fine microstructures are formed in the SLM process [94–98]. The impediment in the SLM process is the surface quality of the built parts, and it is to be improved [99]. The surface roughness of the produced parts affects the mechanical properties. However, the surface quality of as-built products depends upon the selection of suitable parameters and balling phenomenon formed due to the coarse molten metal.

The SLM process is affected by operation parameters and material variables which controlling the processing and strengthen the mechanism of sintered components. These parameters directly affect the part geometry, dimensions of the built part, density, and spatial distribution of pores within a component. Such information is essential in developing strategies for reducing the defect content inside parts [100]. According to spears [101], there are four categories of parameters which are influencing the process. These are laser parameters, properties of powder particles, powder bed properties, and environmental parameters. The SLM process can be managed using parameters such as powder material, build direction, inert gas flow velocity, build platform temperature, and process parameters [102–108]. The process parameters in the Selective Laser Melting process are laser power, laser scanning velocity and strategy, hatch space, and layer thickness [86]. The laser parameters and scanning strategy influence the density of the built parts [109–111]. In the SLM process, the molten metal's stability and the built part's final shape depend upon the laser parameters [112,113].

Generally, metal AM machines manufacturers are designing the machine with a wavelength of 1μm to allow optimal absorption for all metal materials [114]. The laser absorption of aluminum is low compare to other metal materials on a wavelength of 1064 nm. The laser absorption of aluminum is better for wavelengths close to 10μm due to an oxide layer in the powder particles [115]. The power of the laser used in laser sintering and laser melting are different, and this is the

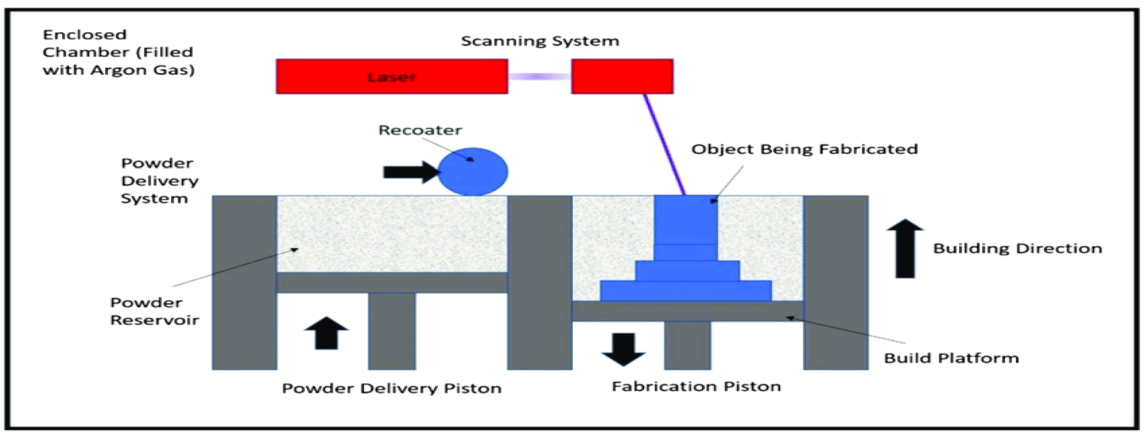

Fig 1 Selective laser melting process [122]

main difference between the two processes. The highest temperature reached in the laser sintering process of aluminum depends upon the alloy type and is generally between 595°C to 625°C. In the case of the laser melting process, the maximum temperature is reached to the melting point temperature of aluminum i.e., more than 660°C [116]. In the SLM process, the melt fluids' mechanics affect the final product's surface quality. The sintering of aluminum powders is complicated due to the natural presence of alumina [117].SLM has become an exemplary fabrication process for aluminum parts since it dramatically shortens the production design and planning. Other significant advantages of the SLM process are less wastage of material [118], topological optimization [119], and re-melting of un-melted powder [120,121].

2.2 Direct Metal Laser Sintering

Direct Metal Laser Sintering (DMLS) is a powder-based 3D printing technique used for manufacturing metal parts. It uses the laser beam to carefully melt the fine metal powder and build it into a fully denser layer-by-layer. This process is entirely automated, and it is used to produce the complex shape parts from the computer-aided design data without the need for special tools [123]. And this method was introduced by EOS GmbH [124]. It is also known as SLM [83], Laser Metal Fusion (LMF) [84], and Laser Beam Melting (LBM) [85]. The moral principle of DMLS is shown in Fig. 2. The blended powders are used as feedstock in the direct metal sintering process. Two types of composite powders are primarily used with low and high melting point temperatures. These powders are fused with the laser beam. The powder with a high melting temperature moderately melts only near the surface during the fusion, whereas the powder with a low melting temperature melts perfectly [125–127]. The rapid cooling and solidification allow production parts with fine microstructure in the DMLS process [128]. This process offers a good balance between the investment costs, range of materials, and part quality, while the finishing quality of parts is still an issue [129]. The surface roughness of the metal AM parts is between 8 to 25 μm (Ra) [129,130], while it depends upon the selection of the processing parameters [131]. Powder material, build direction, inert gas flow speed, build platform temperature, laser power, laser scanning velocity, laser scanning strategy, hatch distance, and layer thickness are the significant parameters that control the quality of the built part in the DMLS process [102–108]. In the DMLS process, the denser parts with the best surface quality can be produced by selecting such processing variables [132].

2.3 Laser Powder Bed Fusion (LPBF)

Laser Powder Bed Fusion (LPBF) is a powder-based 3D printing process used to produce metal parts [134]. Depending on the machine manufacturer, the Laser Powder Bed Fusion is also known as Direct Metal Laser Sintering (DMLS) for EOS Gmbh, laser CUSING for concept laser, Direct Metal Production (DMP) for Phenix (3D system), Selective Laser Melting (SLM) for SLM solutions, Realizer, Matsuura and Renishaw [135,136]. High complex geometries and customized parts are produced in the LPBF process with less wastage of material [137]. The working process of LPBF is shown in Fig. 3. LPBF allow a variety of materials such as copper, steel, nickel, cobalt, titanium, steel, and aluminum alloys for building functional components [138,139]. The complex aluminum

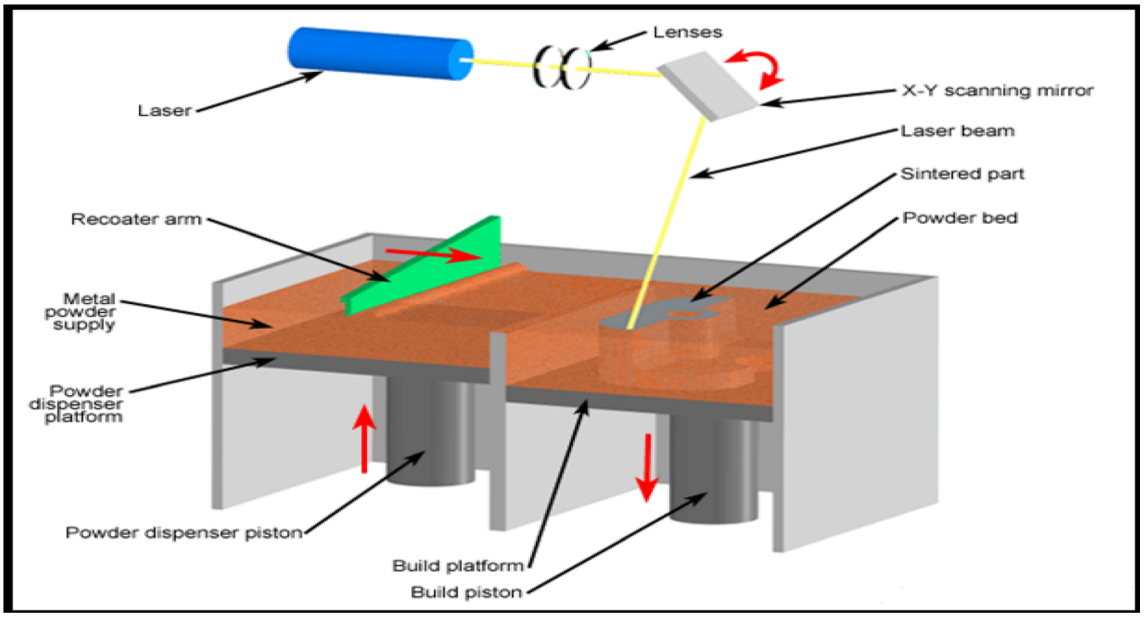

Fig 2 Direct metal laser sintering process [133]

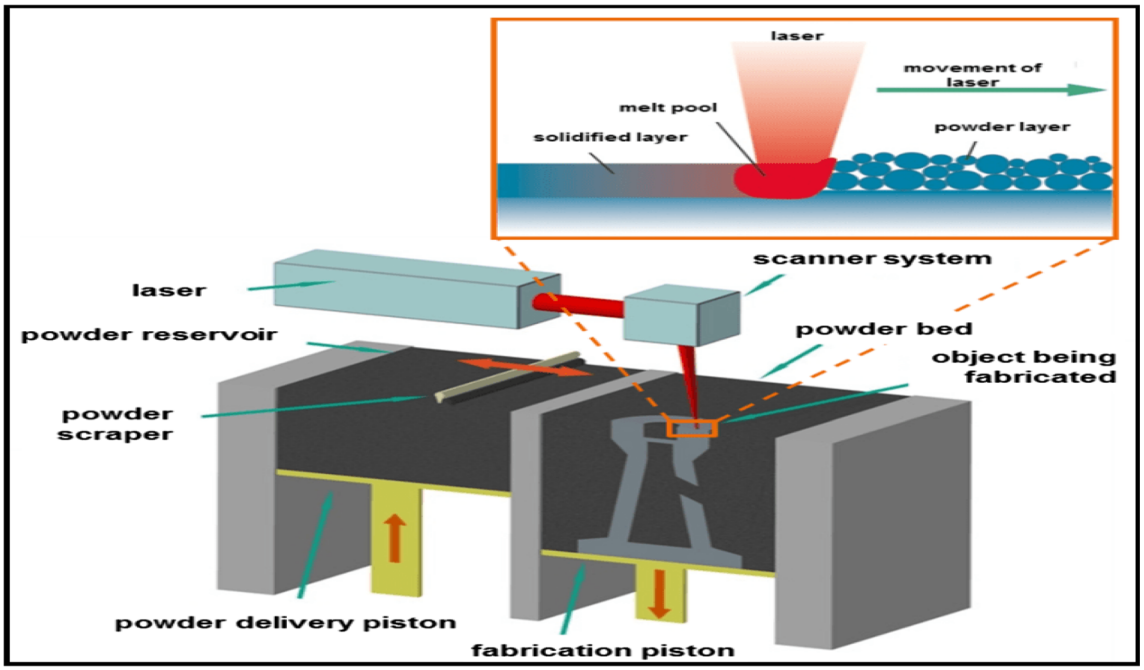

Fig 3 Laser powder bed fusion process [157]

alloys that are not conveniently produced in the casting and deformation process can also be handled successfully in LPBF [140,141]. The parts made in the LPBF are successfully used in jewelry, aerospace, automobile, and biomedical sectors [142–144]. Laser powder, laser scanning velocity, hatch space, the thickness of the layer, and scanning strategy are the significant LPBF processing control parameters [153]. Melting of powder, balling, spatter, and building process affects the final surface roughness of the built components [145–152]. Also, the surface roughness of components produced in the LPBF process depends upon the heat adsorption of powder, reflection, and powder melting [154–156]. The reduction of surface roughness with the LPBF built components can be possible with some post-process treatments.

3 Mechanical and tribological properties of aluminum alloys and their components

The properties like lower absorptivity of the laser and the formation of aluminum oxide layer increased the complexity to additively manufacture the aluminum alloys compared with the steel, titanium (Ti), and nickel (Ni) alloys [158,159]. Al-Si, Al-Mg, Al-Zn-Mg alloy components fabricated by using metal AM techniques such as SLM, LPBF, DMLS [160–162]. Al-Cu and Al-Mn are hindered in their manufacturability by AM due to their inherent high laser reflectivity [163–167]. Al-Cu-Mg alloys are conscious of rupturing due to the presence of copper and magnesium. In the SLM process, cracks are reduced if the laser speed decreases [168]. Al-Cu, Al-Zn alloy components are produced in the SLM process without cracks [165].

3.1 Pure Aluminum

The laser reflectivity of pure aluminum is near 91%, and it is higher than other aluminum alloys [169,170]. The laser absorbing capacity of pure aluminum is enhanced by a coating of high laser absorbing elements on aluminum powder [171]. Cobalt is one of the coating elements due to its material characteristics like high laser absorptivity and high strength via precipitation hardening [172–178]. Geng et al. [179] presented the effect of cobalt phase in 3D printing of aluminum powder in which they found that the laser absorptivity of aluminum powder and its 3D printability improved with the decoration of a little amount of high laser absorbing cobalt nano particles, the powder surface chemical composition modified and it can be roughened due to the homogenous dispersion of Co, internal pores eliminated due to the complete melting. The tensile strength of the aluminum parts produced in additive manufacturing was comparable to medium-strength aluminum alloys..

3.2 Al-Si alloys

The Al-Si alloy components are quickly processed using the SLM technique due to the silicon content among the all-aluminum alloys. It offers superior laser absorption, eliminates cracking, and offers the material adequate flow and weld properties [180]. In addition, Al-Si alloy is used to manufacture heat exchangers, and it is used as filler material [181].

Kimura et al. deliberate the result of silicon percentage in Al-Si alloy parts produced in the Selective Laser Melting Process. They found that the ultimate tensile strength and proof stress of the made parts increases with the silicon percentage rising due to the rise of crystallized phases and the solid solubility of silicon in the aluminum matrix. In contrast, the elongation and thermal conductivity decreased [182]. In the SLM process, higher relative density Al-12Si alloy components is produced by optimizing the laser scanning parameters, and a relative density of more than 99.5% in Al-0Si and Al-20Si samples [182]. Furthermore, the corrosion resistance decreases in SLM Al-Si alloy components due to fine silicon particles [183].

The mechanical and tribological features of AM Al-Si alloy components are reported in Table 1.A very high relative density component was obtained by low scanning velocity, hexagonal scanning strategy, and high laser power. Mechanical properties of built parts are varied with build direction [185,194]. The mechanical properties of 3D printed Al-12Si samples are more than the conventional manufacturing parts [186,192,193]. Heat treatment methods influenced the mechanical characteristics of built components. The ductility of built components increases with hot isostatic pressing and annealing [198–200].

Process and optimum process parameters of additive manufacturing Al-Si alloy parts by different techniques are reported in Table 2. Comparing the process and optimum process parameters of 3D printed Al-12Si alloy parts concerning the relative density, higher relative density obtained at a laser power of 350W, laser scanning velocity of 930 mm/s [185–198]. Comparing the process and optimum process parameters of 3D printed Al-40Si alloy parts concerning the relative density, the maximum relative density obtained at a laser power of 200W, laser scanning velocity of 200 mm/s [201,202].

Mechanical characteristics of Al-Si alloy components are fabricated by casting, and additive manufacturing processes are reported in Table 3. The deformation resistance and maximum strength of Al-Si alloy components produced in the

Table 1 Mechanical and tribological properties of Al-Si alloys [184–203]

Alloy	AM technique	Remarks	Ref
AlSi12	SLM	The built parts exhibit negative strain at room temperature and positive strain rate at high temperature.	[184]
AlSi12	SLM	Higher relative density was obtained at low scanning speed and hexagonal scanning strategy. Yield strength and tensile strength values vary with built orientation.	[185]
AlSi12	SLM	Residual stress is reduced by preheating the powder bed.	[186]
AlSi12	SLM	The ductility is more in the argon, nitrogen atmosphere condition than the helium.	[187]
AlSi12	SLM	The mechanical properties of built parts are more compare to conventional parts.	[188]
AlSi12	SLM	Fatigue behavior improved through base-plate heating.	[189]
AlSi12	SLM	Due to isothermal annealing, the yield strength reduced from 260 MPa to 95 MPa, and the fracture strain increased from 3% to 15 %.	[190]
AlSi12	SLM	The ductility is increased by 25% due to solution heat treatment.	[191]
AlSi12	SLM	The tensile strength of built parts more compares to the casted parts.	[192]
AlSi12	SLM	The strength of the built alloy is more than the conventionally cast alloy.	[193]
AlSi12	SLM	High relative density parts are produced at high laser power.	[194]
AlSi12	SLM	Dendritic morphology increase with increasing laser energy density.	[195]
AlSi12	SLM	The powder drying aspect produces high relative density parts.	[196]
AlSi12	SLM	The highest micro-hardness (about 105 HV) is obtained at a laser power of 210 W.	[197]
AlSi12	SLM	Hot isostatic pressing reduces the strength and increases the fracture strain.	[198]
AlSi12	SLM	The ductility of the built parts increases with annealing heat treatment.	[199]
Al-20Si	SLM	The ductility of the built parts increases with annealing heat treatment.	[200]
AlSi40	SLM	Surface roughness decreases with increasing the energy level. Conversely, high-density parts are obtained at a low energy density.	[201]
AlSi40	SLM	Ductility increases, and ultimate tensile strength decreases due to heat treatment and hot isostatic pressing.	[202]
AlSi25	SLM	Relative density increases with increasing laser power and decreasing the scan speed.	[203]
AlSi50	SLM	Relative density increases with increasing laser power and decreasing the scan speed.	[203]

Table 2 Process and optimum parameters of additive manufacturing Al-Si alloy [185–203].

Alloy	AM technique	Range of parameters				Optimum parameters				Relative density (%)	Ref
		P (W)	v (mm/s)	h(μm)	t (μm)	P (W)	v (mm/s)	h (μm)	t (μm)		
AlSi12	SLM	285	1000-2000	100	40	285	1000	100	40	99.8	[185]
AlSi12	SLM	200	375-2000	150	50	200	500	150	50	98.2	[187]
AlSi12	SLM	350	930	190	50	-	-	-	-	99.7	[189]
AlSi12	SLM	320	1455-1939	110	50	-	-	-	-	99.60	[190]
AlSi12	SLM	100	100–600	100-200	50	100	150	150	50	89.5	[194]
AlSi12	SLM	100–200	70–200	100-500	200-1000	200	120	100	200	77	[195]
AlSi12	SLM	200	500-2000	150	50	-	-	-	-	99	[196]
AlSi12	SLM	120-210	500	50	40	210	500	50	40	96	[197]
AlSi12	SLM	350	930	-	-	-	-	-	-	99.99	[198]
AlSi40	SLM	120-200	30-424	50-300	50	200	200	-	-	99.97	[201]
AlSi40	SLM	200	744 -1993	-	-	-	1300	-	-	99.5	[202]
AlSi25	SLM	125-400	750-2000	120	30	350	1500	120	30	99.95	[203]
AlSi50	SLM	125-400	750-2000	120	30	400	2000	-	-	99	[203]

SLM are more than the casting process and its ductility more in the casting process. Atmosphere condition in additive manufacturing affects the mechanical properties of built pats. Higher deformation resistance and maximum strength of SLM Al-12Si parts are fabricated in argon atmosphere conditions, and high ductility is obtained in nitrogen atmosphere conditions [185–200]

The consequence of pre or post-treating methods on the mechanical properties of AM Al-Si alloy components is reported in Table 4. The deformation resistance and maximum strength of 3D printed Al-12Si alloy components were decreased after heat treatment methods, such as annealing, solution heat treatment, and hot isostatic pressing, and its ductility increases [198–200]. On the other hand, deformation resistance and maximum strength of built components are improved with heat treatment, followed by a hot isostatic pressing [202].

The mechanical characteristics of the 3D printing Al-12Si alloy components are depended upon the atmosphere condition. Figure 4 shows the fracture surface of the SLM Al-12Si components produced using different atmospheric conditions, such as nitrogen (N2), argon (Ar), helium (He). The ductility of the specimens grown in the helium atmosphere condition is less compared to the nitrogen (N2), argon (Ar) atmospheric condition due to the clustering of pores in the samples [187].

Table 3 Comparison of mechanical properties of cast Al-Si alloy and additive manufacturing Al-Si alloy [185–200]

Alloy	AM technique	casting/Die casting			Atmospheres	As Built			Ref
		Yield strength (MPa)	UTS (MPa)	Elongation (%)		Yield strength (MPa)	UTS (MPa)	Elongation (%)	
AlSi12	SLM	55-110	130-230	8-9.5	Argon	225-263	265-365	4-6	[185]
AlSi12	SLM	145	300	2.5	Nitrogen	217-231	357-379	4.2-5.4	[187]
AlSi12	SLM	145	300	2.5	Argon	212-234	347-363	3.6-4.8	[187]
AlSi12	SLM	145	300	2.5	Helium	210-232	299-385	1.1-1.9	[187]
AlSi12	SLM	-	-	-	Argon	260	380	3	[190]
AlSi12	SLM	-	-	-	Argon	102	425	12	[192]
AlSi12	SLM	-	-	-	Argon	266.8-282.8	276.10-310.10	1.9-2.5	[193]
AlSi12	SLM	110	230	9	Argon	197.8-205.2	356.6-365.6	3.9-4.2	[198]
AlSi12	SLM	-	-	-	Argon	239-241	381-389	2.9-3.1	[199]
Al-20Si	SLM	105	162	4.6	Argon	-	506	1.6	[200]

Table 4 Effect of pre or post processing methods on mechanical properties [190–202]

Alloy	AM technique	Built parts			Heat treatment method	After heat treatment			Ref
		Yield strength (MPa)	UTS (MPa)	Elongation (%)		Yield strength (MPa)	UTS (MPa)	Elongation (%)	
AlSi12	SLM	260	380	3	Annealing	95	-	15	[190]
AlSi12	SLM	-	-	-	2 h solution heat treatment	110	190	25	[191]
AlSi12	SLM	197.8-205.2	356.6-365.6	3.9-4.2	Hot isostatic pressing	106.3-110.5	152.1-158.9	17.57-20.83	[198]
AlSi12	SLM	239-241	381-389	2.9-3.1	Annealing at temperature of 573K	135-141	202-212	3.6-4.0	[199]
Al-20Si	SLM	-	506	1.6	Annealing at temperature of 673K	-	252	8.7	[200]
AlSi40	SLM	-	225	-	Heat treatment+ Hot isostatic pressing	-	279	-	[202]

3.3 AlSi10Mg alloy

The AlSi10Mg alloy consists of 10% wt. of Si and 0.3% wt. of Mg, and this composition corresponding to A360 cast alloy [204]. This material has good material characteristics, such as low density, tremendous strength to weight ratio, more strength, high thermal conductivity corrosion resistance, good weld ability compared with other alloys [205–207]. It is used for functional prototypes in aerospace and automotive due to its excellent material characteristics [208,209]. The powder-based AM techniques, such as Selective Laser Melting (SLM), Direct Metal Laser Sintering (DMLS), and Laser Powder Bed Fusion (LPBF) techniques, are widely used for the manufacturing of AlSi10Mg alloy components [267–302]. In the laser additive manufacturing process, the mechanical properties, namely tensile strength [210,211], hardness [210,212], and fatigue [213–217] affected by procedure variables, such as laser scanning speed and power, build direction. The strength and ductility of AlSi10Mg alloy parts are increase in the Selective Laser Melting (SLM) process due to the refined microstructure formed by high cooling rates and synergy between the high power laser beam and powder grains [218–220]. The mechanical properties of SLM AlSi10Mg alloy parts are sensitive to strain rate [221–223]. In the 3D printing process, the deformation resistance of the built components is affected by the process parameters and testing procedure [224–227]. Scanning strategy involves the pores' distribution, crack formation, and microstructure orientation caused by residual stress [228–230]. The fine microstructure is obtained in laser additive manufacturing, and it

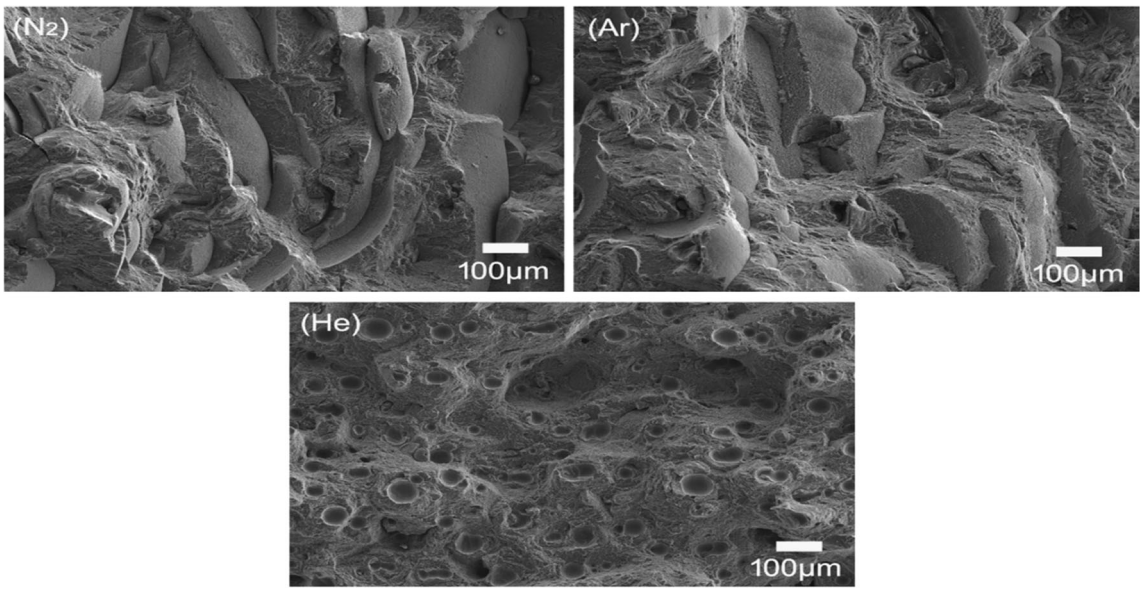

Fig 4 Fracture surfaces of the Al-12Si samples produced using different atmosphere condition [187]

contains the α-Al phase and fibrous Si particles [231]. Size and morphology of eutectic Si phase in AM AlSi10Mg alloy parts influenced the mechanical properties [232,233].

The presence of pores, cores, and partially melted particles in AM components affects the mechanical and fatigue properties. Different porosities were observed in the AM aluminum alloy components. These are classified into powder-induced porosities and process-induced porosities [234]. In AM AlSi10Mg alloys, porosities are located between consecutive layers and melt polls [235]. There are mainly two porosities: oxides [236] and hydrogen [237] formed in SLM AlSi10Mg alloy. The porosity of AM AlSi10Mg alloy is affected by laser power, laser scanning velocity, and hatch distance [209–212]. The relative density of SLM AlSi10Mg alloy components is reached almost 99.8% at a scanning velocity of 500 mm/s, hatch spacing of 50 um, layer thickness of 40 um, and laser power of 100 W. [213]. The lowest porosity components are obtained at a hatch distance of 0.13 mm, laser power 350 W, scanning velocity of 1650 mm/s, and layer thickness of 30 um [214]. Almost 100% relative density parts are fabricated in the SLM process [238]. The pores formed in the SLM AlSi10Mg alloy parts are eliminated using a hot isostatic pressure process [239]. In SLM AlSi10Mg parts, different porosities started to affect the fatigue strength [240]. The fatigue life of the additive manufacturing parts is vital in various industries such as marine, defence, aerospace. The fatigue strength of AlSi10Mg alloy parts produced in SLM is comparable to the cast counterpart A360 [241]. Oxides pores are formed in LPBF AlSi10Mg alloy parts during melting also here, the fatigue inception was continuously accredited to the sub-surface pores specifically [242]. Operation variables are optimized to reduce the process porosity [243]. The build orientation affects the fatigue strength of built parts, showing an impaired behavior for the samples made in the Z direction [244,245]. Achieving good surface quality of parts is challenging in Additive Manufacturing otherwise, which affects the mechanical properties and porosity [246,247]. The surface roughness affects the fatigue strength of the AM AlSi10Mg alloy parts [248,249]. Smoother surface correlated to higher fatigue limits [250]. Required surface roughness depends upon the application, e.g., in biomedical application implants requires smother surface for higher fatigue strength [251,252], and higher surface roughness of the parts causes the corrosion [253], the fuel consumption of the propeller shaft decreased due to improving the performance by reducing the surface roughness [254,255]. The surface quality of the additive manufacturing metal components is in the range of Ra 8-25 μm [256,257]. Two methods that achieved the required surface roughness of the built parts are 1). Post-processing methods, such as mechanical processes to thermal and chemical treatments are available, and selecting the appropriate finishing process depends upon the tolerance, integrity, cost, and lead time [258]. 2) By optimization of operation variables [259]. The horizontal surface roughness of SLM AlSi10Mg alloy parts is reduced by 25% if process parameters are optimized [260]. The surface irregularities of the built components decreases by optimization of operation variables, such as hatch distance, laser power, and scan velocity [261,262]. The surface roughness of the Selective Laser Melting parts is reduced by selecting the relevant processing variables [263]. Laser power and scan speed, layer thickness, hatch spacing, and overlap ratio significantly affect the surface irregularities of laser melting components [264,265]. Orientation of the surface and the presence of a support structure in AM process will also influence the surface quality of the made parts [266].

Mechanical and tribological features of AlSi10Mg alloy components by distinct techniques are reported in Table 5. The mechanical characteristics of AM AlSi10Mg samples are more than conventional manufacturing parts [276,282,290,291], and these are dependent upon the process variables, such as hatch distance, build direction, laser scanning velocity, and layer thickness. Better mechanical properties of build parts occurred at hatch spacing of 190 μm [278]. Build direction affects the deformation resistance. The deformation resistance of components builds in the 0° direction is 8% more than the 90° direction, and the ultimate tensile strength of parts makes in the Z direction more than XY and 45° direction [287,290]. The mechanical properties increase as the build direction increases from 35.5° to 90° [294]. The ultimate tensile strength decreases as the laser scanning velocity increases from 80 to 120 mm/sec [295]. The better mechanical properties occurred at small layer thickness and hatch distance, and the productivity is improved by higher scan speeds [297]. The surface smoothness of the built components depends upon the operation variables. The surface smoothness of the produced components increases with increasing the laser power and increases with increasing the laser energy density [270,271,285]. The surface irregularities of the built components vary with surfaces. The roughness on the top surface is less than the bottom and side surface [277]. The roughness on the bottom surface is more than the top and side surface [281]. Compared to laser power, the hatch distance is the more predominant process parameter that influenced the surface roughness of the built parts [299]. The relative density of the made parts depends upon the operation variables, such as laser power, laser scanning speed, and scan spacing [283]. The porosity of the built parts depends upon the laser energy density. Low energy density causes irregular shapes, and high laser energy density leads to boiling voids [300]

Process and optimum process parameters in AM AlSi10Mg alloy by different techniques are reported in Table 6. Comparing the process and optimum process parameters of AM AlSi10Mg alloy parts concerning relative density, higher relative density parts are produced at a laser power of 370W, laser scanning velocity of 1000 mm/s, and scan

Table 5 Mechanical and tribological properties of AlSi10Mg alloy [267–303]

AM Technique	Remarks	Ref
SLM	The ultimate tensile strength decreases with increasing the porosity percentage. The minimum porosity percentage occurs at an energy density of 60 and 50 J/mm$^{3.}$	[267]
SLM	The dimensions of the built parts are more accurate in the horizontal build direction compared to the vertical direction.	[268]
SLM	The transfer scanning route reduces the residual stress and strain.	[269]
SLM	The surface roughness of the built parts decreased with increasing the laser power.	[270]
SLM	The surface roughness decreases with increasing the laser power at the constant laser energy density.	[271]
SLM	Mechanical properties of horizontal build direction samples more compare to the vertical direction.	[272]
SLM	The electric current enhanced the annihilation process of dislocations during creep. Thus, plastic deformation controlled by dislocation activity.	[273]
SLM	The higher micro hardness obtained due to eutectic Si, as well as Mg_2Si phase.	[274]
SLM	The surface roughness in the inclined plane is more prominent than those of the horizontal plane.	[275]
SLM	The mechanical properties of built parts more compare to casting parts.	[276]
SLM	The roughness on the top surface is less than the bottom and side surface.	[277]
SLM	Hatch spacing affects the mechanical properties. Maximum mechanical properties occurred at hatch spacing of 190 μm.	[278]
SLM	Scanning against the gas flow resulted in higher ultimate tensile strength.	[279]
SLM	The mechanical properties of the build parts are more than that of the HDPC A360F and HDPC A360 T6 alloys.	[280]
SLM	The roughness on the bottom surface is more than the top and side surface.	[281]
SLM	The build parts have better structural properties than the conventional manufacturing parts.	[282]
SLM	The process parameters, such as laser power, scanning speed, and hatch distance, affect the relative density of built parts.	[283]
SLM	Laser scanning speed affects the erosion rate. Too high and too low scanning speeds increase the erosion rate.	[284]
SLM	The surface roughness of the built parts increases with increasing laser energy density.	[285]
SLM	The size of the samples affects the hardness and lowered hardness achieved for smaller-sized samples.	[286]
SLM	Build direction affects the tensile strength. The tensile strength obtained in horizontal build direction specimens is 8% more than vertical build direction specimens.	[287]
SLM	Laser emission affects the microstructure. The finer microstructure obtained in pulsed wave laser emission. Better mechanical properties obtained in continuous-wave laser emission by increasing of thermal load.	[288]
SLM	The mechanical properties of build parts are affected by the size of the strut. These are decreasing with decreasing build diameter.	[289]
SLM	Ultimate tensile strength of parts builds in Z-direction more compare to XY and 45° direction.	[290]
SLM	The tensile strength of the parts built in SLM more than that of the parts builds in casting and elongation more in the casting process.	[291]
SLM	The specific strength of built parts is more than that of metallic and non-metallic micro lattices.	[292]
SLM	In diamond lattice structure, rod diameter and optimum radius affect the mechanical properties.	[293]
SLM	The mechanical properties increase as the build direction increases from 35.5° to 90°	[294]
DMD	The ultimate tensile strength decreases as the scanning speed increase in the range of 80 to 120 mm/sec.	[295]
DMLS	The feed and cutting force decreased by 55% and 47% in the turning operation of sintered parts compared to the casting parts.	[296]
DMLS	The better mechanical properties occurred at small layer thickness and hatch distance, and higher scan speeds improved the productivity.	[297]
DMLS	The micro hardness of the built samples was 24% more than that of the die-cast parts.	[298]
DMLS	Scan speed is the more predominant factor on the surface roughness compared to laser power and hatch distance.	[299]
LPBF	Laser energy density affects the porosity and low energy density, resulting in a lack of fusion voids with an irregular shape. Conversely, high laser energy density leads to boiling voids.	[300]
LPBF	Thin wall structures produced at high laser scan speed and laser power.	[301]
LPBF	The fracture toughness decreases by up to 10% at an angle of 20° between the crack propagation path and the layering.	[302]

Table 6 Process and optimum parameters of additive manufacturing AlSi10Mg alloy [270–299]

AM technique	Range of parameters				Optimum parameters				Relative density(%)	Ref
	P (W)	v (mm/s)	h(μm)	t (μm)	P (W)	v (mm/s)	h (μm)	t (μm)		
SLM	200-370	1000-1500	150-250	30	370	1000	190	30	99.99	[270]
SLM	160-370	150-800	-	30	370	800	-	30	-	[271]
SLM	370	1000	200	30	-	-	-	-	99.98	[273]
SLM	350	930	190	50	-	-	-	-	98.8	[274]
SLM	370	1300	150	40	-	-	-	-	99.88	[275]
SLM	370	1300	160-220	30	370	1300	190	30	-	[278]
SLM	320-380	1550-1750	0.1-0.15	30	350	1650	130	30	99.13	[280]
SLM	320-380	1550-1750	100-150	20-75	350	1650	130	-	99.26	[283]
SLM	370	520-2600	-	-	-	1300	-	-	95.85	[284]
SLM	400	240-340	130	25	-	-	-	-	99	[285]
SLM	300	-	140	25	-	-	-	-	99.5	[288]
SLM	350	1150	170	50	-	-	-	-	99.5	[288]
SLM	370	1500	190	30	-	-	-	-	99.9	[289]
SLM	150	1000	50	50	-	-	-	-	99.96	[290]
SLM	370	1500	150	30	-	-	-	-	99.98	[294]
DMD	1900	80-120	-	-	-	80	-	-	-	[295]
DMLS	280	2000	60	30	-	-	-	-	-	[298]
DMLS	120-190	800-1250	100-200	30	120	900	110	-	-	[299]

spacing of 190 μm, and layer thickness of 30 μm [270–293]. At constant laser power and scan spacing, the relative density of built components increases with increasing scanning velocity [275,294]. The relative density of built features increases as the increasing hatch distance with continuous laser power, laser scanning speed, and layer thickness [289,294].

Mechanical characteristics of AlSi10Mg alloy parts produced by casting and AM techniques are reported in Table 7. The deformation resistance and maximum strength of AlSi10Mg alloy parts produced in the Selective Laser Melting process were more than the casting process. The ductility of AlSi10Mg alloy parts made in the casting process was more than Selective Laser Melting [272–298]. The higher yield strength of the SLM AlSi10Mg was 410 MPa and obtained at a laser power of 370 W, laser scanning velocity of 1300 mm/s, hatch spacing of 190 μm, and layer thickness of 30 μm [276]. The higher ultimate tensile strength of the SLM AlSi10Mg was 473 MPa, obtained at a laser power of 150 W, scanning velocity of 1000 mm/s, hatch distance of 50 μm, and layer thickness of 50 μm [290]. The higher hardness of the SLM AlSi10Mg was 143 HV, obtained at a laser power of 350 W, laser scanning velocity of 1150 mm/s, scan spacing of 170 μm, and layer thickness of 50 μm [288]. The sintered AlSi10Mg parts have some drawbacks in surface finishing, dimensional accuracy, and mechanical properties. These are improved by using post-processing methods. Post-processing methods such as electro less gold plating, electro less silver plating, chemical surface finishing, ultrasonic peening treatment, shot peening, abrasive fluidized bed (AFB), magnetic abrasive machining, hot isostatic pressing, re melting, laser polishing, laser shock peening, stress-relieving, solution heat treatment, T5, T6 heat treatment methods are used to achieve the required surface roughness and to enhance the mechanical features of sintered AlSi10Mg parts.

The mechanical characteristics of 3D printed AlSi10Mg alloy parts later post-processing methods are reported in Table 8. The surface roughness of the built parts decreases with increasing the layer thickness of the gold and silver [303,304]. The surface quality of the made parts is improved after post-processing methods, such as chemical surface finishing, shot peening, abrasive fluidized machining, and magnetic abrasive machining [305,307,310–312]. Ultrasonic and shot peening methods improve the fatigue and hardness of 3D printed AlSi10Mg alloy components [306,308,309].

The mechanical properties of 3D printed AlSi10Mg alloy parts before and after post-refining methods are reported in Table 9. The micro hardness of the 3D printed AlSi10Mg alloy components is improved after post-processing methods, such as ultrasonic peening treatment, shot peening, machining, and machining high and low-intensity shot peening [306–308]. Among the post-refining methods, the micro hardness of the produced components was increased by 28%, and fatigue strength was increased by 33% in shot peening [307,308].

Table 7 Comparison of mechanical properties of cast AlSi10Mg alloy and additive manufacturing AlSi10Mg alloy [272–298]

AM technique	casting/Die casting			As Built			Fatigue strength (MPa)	Hardness (HV)	Ref
	Yield strength (MPa)	UTS (MPa)	Elongation (%)	Yield strength (MPa)	UTS (MPa)	Elongation (%)			
SLM	204.62	255.39	2.75	301.26	401.89	4.30	-	64	[272]
SLM	-	-	-	410	-	-	-	102	[276]
SLM	160	310	4	180	287	14	-	-	[278]
SLM	160-185	300-350	3-5	247	414	6.64	-	149	[279]
SLM	-	-	-	323	396	7.7	-	-	[283]
SLM	-	-	-	-	-	-	-	124.4	[284]
SLM	-	-	-	-	-	-	-	112	[286]
SLM	-	-	-	241.2	379.6	8.1	120	-	[287]
SLM	-	-	-	294	-	-	-	143	[288]
SLM	-	-	-	230.2	355.4	5.51	-	-	[289]
SLM	-	-	-	268	473	7.5	-	128.64	[290]
SLM	-	312.65	12.6	-	445.34	8.68	-	-	[291]
SLM	-	-	-	176.3	360.7	2.92	-	-	[294]
DMLS	-	-	-	-	-	-	-	131	[298]

The surface quality of 3D printed AlSi10Mg alloy components before and after post-processing methods are reported in Table 10. The 3D printed AlSi10Mg parts' surface irregularities were decreased after post-processing methods, such as electroless gold coating, electroless silver coating, shot peening, machining, abrasive fluidized bed grinding process, and magnetic abrasive machining [303–312]. Comparing the surface roughness of built parts was achieved in the electroless gold and silver coating methods, the surface quality of the built components was increased by 41 % in electroless gold coating [303,304]. Comparing the surface roughness of the produced parts was achieved in post-processing methods; the surface roughness of the made components was decreased by 98% in magnetic abrasive machining [303–312].

The mechanical characteristics of 3D printed AlSi10Mg alloy components after the heat treatment process are reported in Table 11. The yield strength and ultimate tensile strength of 3D printed AlSi10Mg alloy components are decreased, and ductility increases after heat treatment methods, such as hot isostatic pressing, re melting, annealing, solution heat

Table 8 Mechanical properties of AlSi10Mg alloy after post processing methods [303–312]

AM technique	Post processing method	Remarks	Ref
LPBF	Electro less gold plating	The surface roughness of built parts decreases with increasing the thickness of the gold.	[303]
SLM	Electro less silver plating	The surface roughness of built parts decreases with increasing the thickness of the silver.	[304]
SLM	Chemical surface finishing	The surface quality improved after the chemical surface finishing.	[305]
SLM	Ultrasonic peening Treatment	The porosity, hardness, and stress corrosion resistance of the built parts are improved.	[306]
SLM	Shot peening	The surface roughness and hardness of the built parts are improved.	[307]
SLM	Shot peening	The fatigue resistance of the built parts is improved.	[308]
SLM	Shot peening	The fatigue resistance of the built parts is improved.	[309]
DMLS	Abrasive fluidized bed	The surface quality of built parts is improved after the abrasive fluidized bed.	[310]
SLM	Abrasive fluidized bed	The surface quality improved by 1 μm at an impact angle of 0°.	[311]
SLM	Magnetic abrasive machining	The surface quality of built parts increases from 7 μm to 0.155 μm after magnetic abrasive machining.	[312]

Table 9 Comparison of mechanical properties before and after post processing method [306–308]

AM technique	Built parts		Post processing method	After post processing method		Ref
	Micro hardness (HV)	Fatigue strength (MPa)		Micro hardness (HV)	Fatigue strength (MPa)	
SLM	116	-	Ultrasonic peening treatment	141	-	[306]
SLM	120	-	Shot peening	154	-	[307]
SLM	120	-	Machining	128	-	[307]
SLM	120	-	Machining high intensity shot peening	147	-	[307]
SLM	120	-	Machining low intensity shot peening	145	-	[307]
SLM	-	60	Shot peening	-	80	[308]

treatment, artificial aging, and T6 heat treatment [314,325–336,346–353]. The porosity of the built parts is improved after hot isostatic pressing, hot isostatic pressing followed by T6 heat treatment, and laser shock peening [315,316,323]. The micro hardness of the produced samples decreases after annealing at 300°C for 2 hours [324], and it is increased after solution heat treatment at 530°C and T6 heat treatment [335]. Higher hardness occurred in solution heat treatment with aging heat treatment [339]. The heat treatment methods affect the relative density of the built parts. The relative density of built components was enhanced after solution heat treatment (SHT) at elevated temperatures 530°C for 2 hours and artificial aging 155°C for 2 hours [341,344]. The corrosion resistance of the built parts increases after the annealing heat treatment [329, 332]. The built components' fatigue resistance decreases after the solution heat treatment, followed by water quenching [343,346].

The comparison of mechanical properties of 3D printed AlSi10Mg alloy components before and after heat treatment methods are reported in Table 12. The yield strength and ultimate tensile strength of built parts were decreased by 56 % and 61% in hot isostatic pressing. The yield strength of the built parts was decreased by 52% in stress relieving and hot isostatic pressing at 500°C. The ductility of the produced parts

Table 10 Comparison of surface roughness before and after post processing methods [303–312]

AM technique	Built parts Surface roughness (Ra) μm	Post processing method	After post processing Surface roughness (Ra) μm	Ref
LPBF	17.03	Electro less gold plating	10	[303]
SLM	17.03	Electro less silver plating	15	[304]
SLM	11.96	Shot peening	5.82	[307]
SLM	11.96	Machining	0.22	[307]
SLM	11.96	Machining high intensity shot peening	5.34	[307]
SLM	11.96	Machining low intensity shot peening	2.05	[307]
SLM	-	Machining	1.75	[309]
SLM	-	Machining +Polishing	0.59	[309]
SLM	-	Shot Peening, steel balls	4.6	[309]
SLM	-	Shot peening, ceramic balls	3.58	[309]
SLM	-	Shot peening, steel balls + removal of 25μm by MP	2.15	[309]
SLM	-	Shot peening, steel balls + removal of 30 mm by EP 40s	1.77	[309]
DMLS	16.72	Abrasive fluidized bed (AFB)	1.5	[310]
SLM	7	Grinding process	0.6	[312]
SLM	7	Magnetic abrasive machining	0.115	[312]

Table 11 Mechanical properties of AlSi10Mg alloy after heat treatment [313–353]

AM technique	Heat treatment method	Remarks	Ref
SLM	Hot isostatic pressing	The irregular-shaped voids are eliminated, and a homogeneous microstructure is obtained.	[313]
SLM	Hot isostatic pressing	The ductility of the built parts increased after the heat treatment.	[314]
SLM	Hot isostatic pressing	The ductility of the built parts increased after the heat treatment.	[315]
SLM	Hot isostatic pressing	The porosity of the built parts reduced after the heat treatment.	[316]
SLM	Hot isostatic pressing + T6 heat treatment	The porosity of the built parts was reduced after hot isostatic pressing, followed by T6 heat treatment	[317]
SLM	Stress relieving +Hot isostatic pressing at 500^0 C	The ductility of the built parts was improved after stress relieving, followed by hot isostatic pressing at 500^0 C.	[318]
SLM	Re melting	The surface quality, relative density, and micro hardness of the built parts were improved after re melting.	[319]
SLM	Re melting	The surface roughness of the built parts decreases after re melting.	[320]
SLM	Re melting	The ductility of the built parts increases after re melting.	[321]
SLM	Laser polishing	The surface roughness of the built parts decreases after laser polishing.	[322]
SLM	Laser shock peening	The porosity and fatigue strength of the build parts are improved after the laser shock peening.	[323]
SLM	Annealing at 300 °C for 2 hours	The micro hardness of the built samples decreased.	[324]
LPBF	Stress relieving at 300^0 C for 2 hrs	The ductility and fatigue resistance of the built parts increased.	[325]
SLM	Heated at 300^0 C for 2 h	The flow stress of the built samples decreased.	[326]
SLM	Stress relieve at 300°C for 2 hours	The ductility of the built parts increased.	[327]
SLM	Heating temperature at 350°C and tempering temperature at 200°C	The ductility of the built parts increased.	[328]
SLM	Stress relieve at 200^0C-300°C for 2 hours	The corrosion resistance increased after stress relieving at at 200^0C-300°C for 2 hours	[329]
SLM	Heating temperature of 320°C for 2 hours and air cooling	The ductility of the built parts increased.	[330]
SLM	Stress relieves 25 to 400°C.	The yield strength and ultimate tensile strength of built parts decreased.	[331]
SLM	Annealing	The corrosion resistance increased.	[332]
SLM	Heating at 300°C/2h + water quench	The yield strength and ultimate tensile strength of built parts decreased.	[333]
SLM	535°C/1h + water quench + 190°C/10h +furnace quench	The yield strength and ultimate tensile strength of built parts decreased.	[334]
SLM	SHT at 530 °C+T6 HT.	The micro hardness of the built parts increased after solution heat treatment at 530 °C and T6 heat treatment.	[335]
SLM	Stress release at 300°C for 2 hours	The ductility of the built parts decreased after stress release at 300°C for 2 hours.	[336]
SLM	Annealing at 300 °C for 2 hours	The mechanical properties are more compared to the casting parts.	[337]
SLM	Solution heat treatment at 550 °C for 2h	The ductility of the built parts increased.	[338]
LPBF	(SHT) at elevated temperatures 530°C for 5 hours and 170°C aging	Higher hardness occurred in solution heat treatment with aging.	[339]
SLM	Solution heat treatment at 540^0C for 2 h.	The surface roughness of the built parts decreased after solution heat treatment at 540^0C for 2 h.	[340]
SLM	(SHT) at elevated temperatures 530°C for 2 hours and artificial aging 155°C for 2 hours	The relative density of built parts increased after solution heat treatment (SHT) at elevated temperatures 530°C for 2 hours and artificial aging 155°C for 2 hours.	[341]
LMD	Solution heat treatment (SHT) for 2 hours	The tensile strength of the built parts was increased.	[342]
SLM	Solution treatment + water quench (ST).	The fatigue strength of the built parts was decreased.	[343]
SLM	SHT at 530°C for 2 hours	The relative density of built parts increased after solution heat treatment (SHT) at elevated temperatures 530°C for 2 hours.	[344]
SLM	T5-like aging at 170^0 C for 90 minutes	The mechanical properties of the build parts	[345]

Table 11 (continued)

AM technique	Heat treatment method	Remarks	Ref
		increased after aging at at 170^0 C for 90 minutes.	
SLM	Solution heat treatment + room temperature water quench + aging	The fatigue resistance of the built parts was decreased.	[346]
SLM	T6 heat treatment	The ultimate tensile strength of the built parts was decreased.	[347]
SLM	T6 heat treatment	The built parts' ultimate tensile strength, yield strength, and fatigue resistance increased after T6 heat treatment..	[348]
SLM	Solution treatment + aging.	Higher mechanical properties occurred in T6 heat treatment.	[349]
SLM	T6 heat treatment	The mechanical properties of the build parts are improved.	[350]
SLM	T6 heat treatment	The ductility of the built parts is improved after T6 heat treatment.	[351]
SLM	T6 heat treatment	The mechanical properties of built parts are more in T6 heat treatment compared to stress-relieving treatment at 160 °C.	[352]
SLM	T6 heat treatment	The ductility of the built parts is improved after T6 heat treatment.	[353]

increases more in stress relieving and hot isostatic pressing than hot isostatic pressing [314,318]. The yield strength and ultimate tensile strength of the built parts decreases less in heating at 300°C for 2h + water quench when compare to the heating at temperature 350°C + tempering at temperature 200°C and heating temperature of 320°C for 2 hours + air cooling [328,331,332]. The ductility of the built parts increases more in heating at a temperature of 320°C for 2 hours + air cooling compares to the heating at 300°C for 2h + water quench and heating at temperature 350°C + tempering at temperature 200°C [328,331,332]. The yield strength and ultimate tensile strength of SLM AlSi10Mg alloy parts were decreased by 39 % and 34% in the solution heat treatment method [338]. The ultimate tensile strength of LMD AlSi10Mg alloy parts was increased by 17% in the solution heat treatment method [339]. The yield strength of SLM AlSi10Mg alloy components decreases less in solution heat treatment followed by artificial aging at 170°C for 12 h than the solution heat treatment and solution heat treatment followed by artificial aging [338,343]. The yield strength and ultimate tensile strength of built parts were decreased by 16 % and 22% in annealing at 300^{o}C for 2 hours [343]. The ductility of the built parts was increased by 46% in annealing at 300^{o}C for 2 hours [343]. The ultimate tensile strength of the SLM AlSi10Mg alloy components decreases less in T6 heat treatment than the T2 heat treatment, and T6 heat treatment followed by T2 heat treatment method [347]. Built parts' yield strength and ultimate tensile strength were increased by 26 % and 20% in T6 heat treatment [348,350]. Among the heat treatment methods, the yield strength and ultimate tensile strength of built parts decrease less in the annealing method. The yield strength and ultimate tensile strength of built components improved in the T6 heat treatment method. The micro hardness of the produced parts decreases in hot isostatic, annealing, and heating temperature of 320°C for 2 hours and air cooling, solution heat treatment, and solution heat treatment followed by artificial aging. Among the heat treatment methods, the micro hardness of the built parts decreases less in annealing at 300°C for 60s [314,324,331,338,353], and it is increased in re melting, RT+170°C for 2 hours, T5-like aging at 170°C for 90 minutes, and T6 heat treatment and, increases more in T6 heat treatment [319,339,345,348]. [319,339,345,348].

The surface roughness of 3D printed AlSi10Mg alloy parts before and after heat treatment methods was reported in Table 13. The surface quality of the 3D printed AlSi10Mg was increased after heat treatment methods, such as re melting, laser polishing, solution heat treatment, and a combination of solution heat treatment and artificial aging. Among the heat treatment methods, the surface irregularities of the built components were decreased by 92% in laser polishing [319,320,322,340].

3.4 AlSi10Mg-200C Alloy

The DMLS AlSi10Mg-200C alloy parts are used in different industrial sectors like medical [354] and aerospace [355]. In the DMLS AlSi10Mg-200C process, the elongation of horizontally built parts is more than vertical made parts due to the recycled powder process, and this process does not influence the microstructure and mechanical characteristics [356]. Compare to the casting process, the corrosion resistance of AlSi10Mg-200C alloy components increases in the DMLS method. In the DMLS technique, the AlSi10Mg-200C alloy parts are made with fine microstructure due to the uniform distribution of Si particles [357]. The surface quality of DMLS AlSi10Mg-200C alloy parts improved through the bead blasting method. The attained surface quality is high compared to the pieces produced in the DMLS method [358]. The surface roughness of the AlSi10Mg-200C parts made by DMLS affects fatigue growth. The fatigue cracks initiation and cracks elongation in AM parts due to sub cracks, pores, and defects [359]. The fatigue life of AlSi10Mg-200C parts produced in the DMLS method increased as the surface

Table 12 Comparison of mechanical properties before and after heat treatment methods [314–353]

AM technique	Built parts				Heat treatment method	After heat treatment				Ref
	Yield strength (MPa)	UTS (MPa)	Elongation (%)	Hardness		Yield strength (MPa)	UTS (MPa)	Elongation (%)	Hardness	
SLM	268	474	7.8	130	Hot isostatic pressing	116	185	20.6	65	[314]
SLM	241	384	6	-	Stress relieving and hot isostatic pressing at 250^0 C	186	233	22	-	[318]
SLM	241	384	6	-	Stress relieving and hot isostatic pressing at 500^0 C	115	141	35	-	[318]
SLM	-	-	-	117.7	Re melting	-	-	-	121.6	[319]
SLM	-	377	5.3	-	Re melting	-	368	8.3	-	[321]
SLM	250	-	-	131	Annealing at 300 °C for 60 s.	-	-	-	105	[324]
SLM	-	-	-	-	Annealing at 300 °C for 2 hours	-	-	-	-	[324]
SLM	-	-	-	-	Annealing 530 °C, for 60 seconds	-	-	-	-	[324]
SLM	202.8	282.6	2.5	95	Annealing at 300°C for 2 hours	148.5	231	3.4	75	[327]
SLM	-	387.4	3.22	-	Heating at temperature 350°C + tempering at temperature 200°C	-	168.8	1.95	-	[328]
SLM	-	443	-	-	Annealing	-	448	-	-	[329]
SLM	-	-	-	-	Annealing at 300°C for 2 hours	-	346	-	-	[329]
SLM	287	413	5.5	134	Heating temperature of 320°C for 2 hours and air cooling	142	234	13.4	76	[331]
SLM	270.01	446.3	8.09	-	Heating at 300°C/2h + water quench	169.9	273.18	15.27	-	[332]
SLM	270.01	446.3	8.09	-	535°C/1h + water quench + 190°C/10h +furnace quench	164.19	213.65	11.08	-	[332]
SLM	-	-	-	97	Annealing at 300 °C for 2 hours	-	-	-	78	[335]
SLM	-	-	-	97	SHT at 530 °C	-	-	-	62	[335]
SLM	-	-	-	97	SHT at 530 °C+T6 HT.	-	-	-	115	[335]
SLM	-	-	-	-	Annealing at 300 °C for 2 hours	212	325	14.2	-	[337]
SLM	322.17	434.3	5.3	132.55	SHT at 450 °C for 2h	196.58	282.36	13.4	95.65	[338]
SLM	-	-	-	-	Solution heat treatment	90.52	168.11	23.7	63.55	[338]
LPBF	-	-	-	134	Solution heat treatment (SHT) at elevated temperatures 530°C for 5 hours	-	-	-	75	[339]
LPBF	-	-	-	134	SHT+170°C	-	-	-	104	[339]
LPBF	-	-	-	134	RT+170°C for 2 hours	-	-	-	149	[339]
LMD	-	292	-	-	Solution heat treatment for 2 hours	-	342	-	-	[342]
SLM	319	477.5	4	-	Annealing at 300°C for 2 h	266	369	7.5	-	[343]
SLM	319	477.5	4	-	Solution heat treatment followed by artificial ageing	151	253	-	-	[343]
SLM	319	477.5	4	-	SHT followed by artificial ageing at 170°C for 12 h (T6)	197.5	-	-	-	[343]
SLM	288	414	5.6	138	T5-like aging at 170^0 C for 90 minutes	-	-	-	145	[345]
SLM	-	312	4	-	T6 heat treatment	-	267	9	-	[347]
SLM	-	312	4	-	T2 heat treatment	-	171	12	-	[347]
SLM	-	312	4	-	T6 +T2 heat treatment	-	162	21	-	[347]
SLM	210	325	-	136	T6 heat treatment	285	345	-	178	[348]
SLM	-	382	2.3	125	Annealing at 300 °C	-	220	-	-	[349]
SLM	-	-	-	-	Solution heat treatment followed by artificial ageing	248	307	9.3	101	[349]
SLM	159	160	1.59	107	T6 heat treatment	171	192	1.77	109	[350]
SLM	-	-	-	-	Heating 160 ^{0}C for 4 h	321	471	8.6	-	[351]
SLM	-	-	-	-	T6 heat treatment	243	323	15.3	-	[351]
SLM	-	-	-	-	Heating of plat form at 160 ^{0}C	248	386	8.6	-	[351]

Table 12 (continued)

AM technique	Built parts				Heat treatment method	After heat treatment				Ref
	Yield strength (MPa)	UTS (MPa)	Elongation (%)	Hardness		Yield strength (MPa)	UTS (MPa)	Elongation (%)	Hardness	
SLM	255	377	2.2	-	Stress-relieving treatment at 160 °C/5 h)	158	256	9.9	-	[352]
SLM	-	-	-	-	T6 heat treatment	210	284	4.9	-	[352]
SLM	268	333	1.4	125	1h SHT+ 6 h AA	239	292	3.9	100	[353]
SLM	-	-	-	-	6h SHT+ 7 h AA	-	-	-	103	[353]

roughness reduced [360]. The surface roughness of the AM parts is diminished with the laser re melting process [361]. Various process parameters control the surface quality of final components, and the ANOVA method is used to study the effect of varying process parameters on the absolute quality of the specimens [362,363].

3.5 A357 Alloy

The AlSi7Mg (A357) alloy is a suitable material to be used in different industrial applications. In the automotive industry, A357 alloy is used to produce blocks, cylinder heads, and suspension systems due to having good mechanical features, more specific strength, significant corrosion, and fatigue resistance [364]. Takahiro et al. studied the microstructure and mechanical characteristics of A356 alloy parts produced by Selective Laser Melting under the optimum irradiation condition. They concluded the mechanical characteristics of built components are more than the casting parts due to fine dendritic cell microstructures; after the annealing (T5) process, ultimate tensile strength, yield strength decreases and ductility increases from 15% to 30%, and almost 100 % relative density achieved [365]. The relative density of SLM A357 alloy components increases with increasing the laser power at a particular laser scanning velocity. At constant hatch distance and layer thickness, the maximum relative density of 99.68% was achieved inbuilt parts exact a laser power of 300W, laser scanning velocity of 2000 mm/s with 35°C substrate temperature. Substrate temperature affects the relative density; at 200°C, the maximum relative density of built components is achieved at 370 W laser power and 2000 mm/s laser scanning velocity. The maximum strength of the A357 alloy obtained in the SLM process is more than that of the T6-casting process [366]. The building platform temperature affects the ultimate tensile strength, yield strength. Maximum occurs at build platform temperature of 140°C and 170°C due to it can act as an aging process and activates the precipitation of reinforcing phases.

The higher hardness-built parts were obtained in the SLM process with a platform temperature of 100°C by applying a heat treatment at 170°C for 3h [367]. During the fabrication of A357 alloy parts by Selective Laser Melting, a very few gas pores are formed; these are increases after the solution heat treatment at 543°C. Enlargement of gas pores is reduced by pre-drying of powder [368]. Different heat treatments affect the yield strength and elongation of the SLM A357 alloy. The higher yield strength is obtained in artificial aging when compared to stress relieving and solution heat treatment. Higher ductility parts are obtained in the stress-relieving than the artificial aging and solution heat treatment. The mechanical features of SLM A357 alloy components are more than the casting components [369]. The fatigue strength of LPBF A357 parts 60 MPa was achieved at $2x10^6$ cycles [370]. Higher

Table 13 Comparison of surface roughness before and after heat treatment [319,320,322,340].

AM technique	Built parts Surface roughness (Ra) μm	Post processing method	After post processing Surface roughness (Ra) μm	Ref
SLM	13.34	Re melting	9.94	[319]
SLM	20.67	Re melting	11.67	[320]
SLM	8.7	Laser polishing	0.66	[322]
SLM	4.23	Solution heat treatment	3.69	[340]
SLM	4.23	Solution heat treatment followed by artificial ageing	4.51	[340]

density and hardness SLM A357 alloy parts obtained with powder pre-treated at 60°C than the powder pre-treated at 200°C due to the presence of Al_2O_3 in the powder pre-treated at 200°C [371]. In the 3D printing techniques, the build platform condition affects the mechanical properties, and the tensile strength of built parts increases with increasing the build form temperature from 0°C to 90°C and this tensile strength more compare to post-build heat treatment methods such as stress relieving, followed by solution heat treatment and artificial aging [372]. The LPBF process successfully produced the high relative density A357 alloy parts. Heat treatment affects ductility. The ductility of LPBF A357 parts increases with stress-relieving, and its firmness, durability decrease. The micro hardness of the built parts improved by stress-relieving, followed by T6 treatment and aging [373].

The process parameters used in AM of A357 alloy parts by different techniques are reported in Table 14. Comparing the process and optimum process parameters of SLM A357 alloy parts concerning the relative density, higher relative density obtained at a laser power of 300W, the laser scanning velocity of 2000 mm/s, hatch distance of 100 μm, and layer thickness of 30 μm [365,366,369,371,373].

The mechanical features of 3D printed A357 alloy parts before and after heat treatment are reported in Table 15. The yield strength and ultimate tensile strength of 3D printed A357 alloy parts were decreased, and their ductility increases after heat treatment methods, such as annealing, solution heat treatment, artificial aging, and T6 heat treatment [365–367,373]. Among the heat treatment methods, the ultimate strength of the built parts was increased by 7% in natural aging at 160°C-8h. The yield strength of the produced parts was increased by 7% in solution heat treatment, followed by artificial aging. The ductility of the built components was increased by 98% in stress relieved 300°C -2h [369].

3.6 AlSi10Mg composites

Aluminum-matrix composites (AMCs) are extensively employed in aerospace, automotive, microelectronics, and architectural construction due to their excellent metallic characteristics, such as excellent ductility, high hardness, excellent durability, and tremendous specific strength, admirable thermal and electric conductivities, and ceramic properties [374–376]. In the traditional manufacturing process, infiltration, powder metallurgy, spray casting, and stir casting methods are used to fabricate aluminum matrix composites. Heterogeneous distribution of reinforcement, the significant formation of porosity, and the poor wet ability between matrix and reinforcement are the difficulties in infiltration, powder metallurgy, and spray casting methods. The advantages of the stir casting process are that it can break the Al-oxide layer and produce the relatively homogeneous ceramic reinforced aluminum composite parts. The disadvantages are it needs expensive and dedicated tools and complicated preprocessing and post-processing treatments, which causes the complexity of the process [377,378]. Powder-based additive manufacturing methods, such as Selective Laser Melting, Direct Metal Laser Sintering, and Laser Powder Bed Fusion, successfully fabricates the aluminum metal matrix composites. In laser additive manufacturing, a high laser beam generates a high temperature, breaking the Al-oxide layer [379,380]. Microstructure homogeneity occurred due to the marangoni convection and response capillary effort for liquid flow. The laser-make molten pool is characterized by highly rapid melting/solidification [381–384]. The manufacturing flexibility of aluminum alloy parts in 3D printing is less due to their high heat conduction and fewer lasers absorptive to the laser beam. The laser absorbent of aluminum alloy to the laser beam is only 9% [385]. The laser absorption of ceramic particles is high compared to aluminum alloys. Thermal characteristics and stability of the molten pool of the aluminum alloy improved with the addition of ceramic materials due to the complete melting [386–387].The composites produced in the additive manufacturing process showing superior mechanical properties [388–390]. The aluminum metal matrix composites fabricated in a powder-based additive manufacturing process show enhanced wear resistance [391]. The AlSi10Mg alloy is mainly employed in automobile and aerospace sectors due to its excellent weld and harden ability, corrosion resistance, thermal conductivity, and good anti-oxidation properties

Table 14 Process and optimum parameters of additive manufacturing A357 Alloy [365,366,369,371,373].

Alloy	AM technique	Range of parameters				Optimum parameters				Relative density (%)	Ref
		P (W)	v (mm/s)	h (μm)	t (μm)	P (W)	v (mm/s)	h (μm)	t (μm)		
AlSi7Mg0.3	SLM	200-370	400-3000	-	30	-	-	-	-	99.80	[365]
A357	SLM	100-370	500-5000	100	30	300	1000-2000	100	30	99.68	[366]
A357	SLM	750	1100	-	-	-	-	-	-	99.40	[369]
A357	SLM	70-170	500-1200	70	30	170	500	-	-	99.10	[371]
A357	LPBF	195	600-1200	100-200	30	-	1200	100	-	99.94	[373]

Table 15 Comparison of mechanical properties before and after heat treatment method [365–373]

Alloy	AM technique	Before heat treatment				Heat treatment method	After heat treatment				Ref
		Yield strength (MPa)	UTS (MPa)	Elongation (%)	Hardness (HV)		Yield strength (MPa)	UTS (MPa)	Elongation (%)	Hardness (HV)	
A357	SLM	200	400	12-17	-	Annealing(T5)	125	200	30	-	[365]
A357	SLM	-	426.4	9.8	-	Subtract temperature 35°c	-	307.7	7.1	-	[366]
A357	LPBF	-	-	-	-	Building plat form temperature-100° C	249	392	5.4	-	[367]
A357	LPBF	-	-	-	-	Building plat form temperature-140° C	287	413	5.1	-	[367]
A357	LPBF	-	-	-	-	Building plat form temperature-170° C	295	406	4.1	-	[367]
A357	LPBF	-	-	-	-	Building plat form temperature-190° C	250	364	4.5	-	[367]
A357	SLM	225	375	7.8	-	Direct ageing at 160° C -8 h	280	400	5.6	-	[369]
A357	SLM	225	375	7.8	-	Stress Relieved 300° C -2h	125	220	15.5	-	[369]
A357	SLM	225	375	7.8	-	Solution heat treatment and artificial ageing	240	280	6.4	-	[369]
A357	LPBF	245	386	5.2	119	Stress-relieved	189	288	8.2	80	[373]
A357	LPBF	-	-	-	119	Stress-relieved + T6+ ageing at 170 C for 3 h	249	307	5.1	116	[373]

[392–394]. Meanwhile, the mechanical and tribological characteristics of 3D printed AlSi10Mg alloy components are improved with the reinforcement particles listed in Table 16, and their effects are reported in Table 17.

The list of reinforcing particles added to the 3D printed AlSi10Mg alloy components is reported in Table 16. The AIN, Al_2O_3, Fe_2O_3, TiB_2, nano TiB_2, Grapheme, nano TiC, CNT, and TiN/ AlSi10Mg composites were successfully fabricated by powder-based additive manufacturing techniques.

The mechanical and tribological characteristics of SLM AlSi10Mg composite components produced by 3D printing techniques are reported in Table 17. The wear resistance of

Table 16 List of reinforcement particles added to the AlSi10Mg alloy [395–409]

S. No	Aluminum Alloy	Reinforcement	Weight Ratio	AM Technique	Ref
1	AlSi10Mg	AIN	90 : 10	SLM	[395]
2	AlSi10Mg	AIN	99 : 1	SLM	[396]
3	AlSi10Mg	AIN	98 : 2	SLM	[397]
4	AlSi10Mg	Al_2O_3	80 : 20	SLM	[398]
5	AlSi10Mg	Al_2O_3	85 : 15	SLM	[399]
6	AlSi10Mg	Fe_2O_3	85 : 15	SLM	[400]
7	AlSi10Mg	TiB_2	90 :10	DMLS	[401]
8	AlSi10Mg	TiB_2	99 :1	DMLS	[401]
9	AlSi10Mg	TiB_2	99:1	SLM	[402]
10	AlSi10Mg	Nano TiB_2	7 volume%	SLM	[403]
11	AlSi10Mg	Al-coated Grapheme	99 :1	SLM	[404]
12	AlSi10Mg	Grapheme	99 :1	SLM	[404]
13	AlSi10Mg	Grapheme	99.99 :0.1	LPBF	[405]
14	AlSi10Mg	Grapheme	99.98 :0.2	LPBF	[405]
15	AlSi10Mg	Nano Tic	97 : 3	SLM	[406]
16	AlSi10Mg	CNT	99.95 : 0.5	SLM	[407]
17	AlSi10Mg	CNT	49.5 : 0.5	SLM	[408]
18	AlSi10Mg	TiN	98 : 2	SLM	[409]

Table 17 Mechanical and tribological properties of AlSi10Mg composite material [395–409]

Aluminum composite	AM technique	Remarks	Ref
sAIN/AlSi10Mg	SLM	The distribution of AIN in AIN/AlSi10Mg composite changes from severe aggregation to homogeneous distribution as the scanning velocity increases from 100 to 400 mm/sec.	[395]
AIN/AlSi10Mg	SLM	The wear resistance of built parts increased.	[396]
Al_2O_3/AlSi10Mg	SLM	The wear resistance of the built parts decreased with increased load.	[398]
Al_2O_3/AlSi10Mg	SLM	The loss rate of Al_2O_3 increased with increased laser energy density.	[399]
Fe_2O_3/AlSi10Mg	SLM	The composite is more rigid than the corresponding casting Al alloy.	[400]
TiB_2/AlSi10Mg	DMLS	The wear rate of TiB2/AlSi10Mg composite is higher than the casting AlSi10Mg alloy.	[401]
TiB_2/AlSi10Mg	SLM	The mechanical properties and laser absorptivity of AlSi10Mg alloy improved with the addition of TiB2 particles.	[402]
Nano TiB_2/AlSi10Mg	SLM	The mechanical properties and laser absorptivity of AlSi10Mg alloy improved with the addition of nanoTiB_2 particles	[403]
Al-coated graphene/AlSi10-Mg	SLM	Higher tensile strength was obtained when compared with alloy.	[404]
Graphene/AlSi10Mg	PBF	The yield strength and hardness of the AlSi10Mg alloy increased with the addition of graphene.	[405]
Nano TiC/AlSi10Mg	SLM	The tensile strength of the alloy increased.	[406]
CNT/AlSi10Mg	SLM	The ultimate tensile strength of the AlSi10Mg alloy increased with 0.5 wt % of carbon nanotube particles.	[407]
CNT/AlSi10Mg	SLM	The hardness of the AlSi10Mg alloy is improved with the addition of carbon nanotube particles.	[408]
TiN/AlSi10Mg	SLM	The hardness of the AlSi10Mg alloy is improved with the addition of TIN particles.	[409]

SLM AlSi10Mg alloy increases with Al_2O_3 and AIN particles [396,398]. The hardness of SLM AlSi10Mg alloy was improved by adding Fe_2O_3, CNT, and TIN particles [400,408,409]. The mechanical properties of SLM AlSi10Mg alloy enhanced with TiB_2, Grapheme, nano TiC, CNT, and TiN particles [402–407].

4 Conclusions

The powder-based manufacturing techniques, such as Selective Laser Melting (SLM), Laser Powder Bed Fusion (LPBF), Direct Metal Laser Sintering (DMLS), are successfully employed for the manufacturing of Al-Si alloys and aluminum metal matrix composite components. Compared to traditional manufacturing, the mechanical features of the built components are improved in additive manufacturing and have some drawbacks in surface finishing and dimensional accuracy, which are improved by post-processing and heat treatment methods. The following conclusions are drawn from the extensive review and presented as follows..

1. The 3D printability of aluminum powder improved by decorating a small amount of high laser absorbing cobalt nano particles. The maximum strength of AM aluminum components is close to medium strength aluminum alloys components.
2. The 3D printability of Al-Si alloy parts is more than all-aluminum alloy parts due to having silicon content, which gives higher laser absorption. The yield strength and ultimate tensile strength of the 3D printed Al-Si alloy parts are more than the conventionally cast alloy parts. Its ductility improved through the heat treatment process, such as annealing and hot isostatic pressing. Higher relative density parts were obtained at high laser power and by powder drying aspect. The relative density of AlSi25 and AlSi50 alloy components increases with increasing laser power and decreasing the laser scan speed..
3. The yield strength and ultimate tensile strength of the 3D printed AlSi10Mg alloy parts are more than the conventionally cast AlSi10Mg alloy parts. Its ductility improved through hot isostatic pressing, annealing, solution heat treatment, T6 and T2 heat treatment methods. The surface roughness of the built pats decreased by post-processing and heat treatment methods. Among the heat treatment methods, the laser polishing method reduces the surface roughness by 92%, and in the post-processing methods, the magnetic abrasive machining process decreases the

surface roughness by 98%. Hot isostatic pressing and laser shock peening are used to reduce the porosity of the built parts.

4. The tensile and yield strength of the SLM A357 build parts is more than the casting parts, and its ductility improved in annealing. The higher yield strength is obtained in artificial aging when compared to stress relieving and solution heat treatment. The ductility of the 3D parts was obtained in the stress-relieving more when compared with the artificial aging and solution heat treatment.
5. Powder-based additive manufacturing techniques are successfully used to manufacture the AlSi10Mg metal matrix composites. In addition, the reinforcements such as AIN, Al_2O_3, Fe_2O_3, TiB_2, CNT, TiN particles are used to enhance the mechanical properties and wear resistance of the 3D printed AlSi10Mg alloy components.

The metal 3D printing methods are a new manufacturing process used to manufacture complex rapid prototyping tools with design flexibility. The additive manufacturing techniques allow the designers to apply multi-material topology optimization of components used in medicine such as dental prostheses, orthopedic implants such as lightweight scaffold implants structures, aerospace industry, and automotive and power sectors. Small batch sizes are produced in additive manufacturing at a reasonable cost. In the automobile sector, 3D printing allows designers to design and fabricate lightweight components to reduce fuel consumption and the emission of CO_2. The time gap between design and manufacturing is reduced by reducing the wastages and replacing the process sequence with a single process in additive manufacturing. The potential applications of metal 3D printing methods are expected to design, fabricate, and repair components used in the aerospace, medical, automotive, and power sectors.

Authors Contributions •**Bheemavarapu Subba Rao**: Conceptualization, Methodology, Data collection, Writing-review, and editing.

•**Thella Babu Rao**: Review, Editing, and Supervision.

•All authors have read and agreed to publish a version of the manuscript.

Funding This research received no external funding

Data Availability This article is a review article. All Reference papers are available.

Declarations

This article is a review article

Consent to participate 'Not applicable'

Consent for Publication 'Not applicable'

Conflict of Interest The authors declare that they have no conflict of interest. This review article does not contain any studies with human participants or Animals performed by any of the authors.

References

1. Hull, C.W., Apparatus for production of three-dimensional objects by stereo lithography. Google Patents, (1986)
2. C. Brecher, Integrative Production stechnikfürHochlohnländer, Springer, (20011) 1781
3. Emmelmann C, Kranz J, Herzog D, Wycisk E (2014) Laser additive manufacturing of metals. In: Schmidt V, Belegratis MR (eds) Latest technology in biomimetics. Springer, Heidelberg, pp 143–162
4. Zhang S, Wei QS, Cheng LY, Li S, Shi YS (2014) Effects of scan line spacing on pore characteristics and mechanical properties of porous Ti6Al4V implants fabricated by selective laser melting. Mater Des 63:185–193
5. Atzeni E, Salmi A (2012) Economics of additive manufacturing for end-usable metal parts. Int J Adv Manuf Technol 62(2012): 1147–1155
6. Chen F, Wu J-M, Wu H-Q, Chen Y, Li C-H, Shi Y-S (2018) Microstructure and mechanical properties of 3Y-TZP dental ceramics fabricated by selective lasersintering combined with cold isostatic pressing. Int J Lightweight Mater Manuf 1:239–245
7. Qiu Z, Yao C, Feng K, Li Z, Chu PK (2018) Cryogenic deformation mechanism of CrMnFeCoNi high-entropy alloy fabricated by laser additive manufacturing process. Int J Lightweight Mater Manuf 1:33–39
8. Ma Z, Lin J, Xu X, Ma Z, Tang L, Sun C, Li D, Liu C, Zhong Y, Wang L (2019) Design and 3D printing of adjustable modulus porous structures for customized diabetic foot insoles. Int J Lightweight Mater Manuf 2(1):57–63
9. K.A. Al-Ghamdi, Sustainable FDM additive manufacturing of ABS components with emphasis on energy minimized and time efficient lightweight construction, Int. J. Lightweight Mater. Manuf. .2(4) (2019) 338-345
10. Atzeni E, Iuliano L, MInetola P, Salmi A (2010) Redesign and cost estimation of rapid manufactured plastic parts. Rapid Prototyp J **16**(5):308–317
11. Atzeni E, Salmi A (2012) Economics of additive manufacturing for end-usable metal parts. Int J Adv Manuf Technol **62**(9-12): 1147–1155
12. Mellor S, Hao L, Zhang D (2014) Additive manufacturing: A framework for implementation. Int J Prod Econ **149**:194–201
13. D. Herzog, V. Seyda, E. Wycisk, C. Emmelmann, additive manufacturing of metals, Acta Mater. 117 (2016) 371–392
14. Tolosa I, Garciandía F, Zubiri F (2010) Study of mechanical properties of AISI 316 stainless steel processed by "selective laser melting", following different manufacturing strategies. Int J Adv Manuf Technol 51(5–9):639–647
15. K. Guan, Z. Wang, M. Gao, X. Li, X. Zeng, Effects of processing parameters on tensile properties of selective laser melted 304 stainless steel, Mater. Des. 50 (2013)581–586.
16. Vrancken B, Thijs L, Kruth J-P, Van Humbeeck J (2012) Heat treatment of Ti6Al4V produced by Selective Laser Melting: microstructure and mechanical properties. JAlloy Compd 541(15): 177–185
17. X. Gong, T. Anderson, K. Chou, A study of the microstructural evolution during selective laser melting of Ti-6Al-4V, Acta materialia.58(9) (2010) 3303-3312
18. Jia Q, Gu D (2014) Selective laser melting additive manufacturing of Inconel 718 super alloy parts: densification, microstructure and properties. J Alloys Compd 585:713–721

19. Kanagarajah P, Brenne F, Niendorf T, Maier H (2013) Inconel 939 processed by selective laser melting: Effect of microstructure and temperature on the mechanical properties under static and cyclic loading. Mater Sci Eng A 588:188–195
20. Kumar S, Pityana S (2011) Laser-based additive manufacturing of metals. Adv Mater Res 227:92–95
21. Kumar S. Selective Laser Sintering: Recent Advances. In: 4th Pacific International Conference on Applications of Lasers and Optics. Wuhan-China, 617(2010).
22. Khan M, Dickens PM (2008) Processing parameters for Selective Laser Melting (SLM) of gold. In: Proceedings of Solid Freeform Fabrication symposium:278–279
23. Louvis E, Fox P, Sutcliffe C (2011) Selective laser melting of aluminum components. J Mater Process Technol 211(2):275–284
24. Thijs L, Kempen K, Kruth J-P, Humbeeck JV (2013) Fine-structured aluminum products with controllable texture by selective laser melting of pre-alloyed AlSi10Mgpowder. Acta Mater 61:1809–1819
25. Aboulkhair NT, Everitt N, Ashcroft I, Tuck C (2014) Reducing porosity in AlSi10Mg parts processed by selective laser melting. Addit Manuf 1:77–86
26. Kumar S, Kruth JP (2010) Composites by rapid prototyping technology. Mater Des 31(2):850–856
27. Ghosh SK, Saha P, Kishore S (2010) Influence of size and volume fraction of SiC particulates on properties of ex situ reinforced Al-4.5Cu-3Mg metal matrix composite prepared by direct metal laser sintering process. Mater. Sci. Eng. A 527(18–19):4694–4701
28. Vaezi M, Chianrabutra S, Mellor B, Yang S (2013) Multiple material additive manufacturing, Part1: a review. Virtual and Phys Prototype 8:19–50
29. Herderick E (2015) Progress in additive manufacturing. J Mater 67:580–581
30. V. Matilainen, H. Piili, A. Salminen, T. Syvänen, O. Nyrhilä, Characterization of Process Efficiency Improvement in Laser Additive Manufacturing, Phys Procedia 56(0) (2014) 317-326.
31. B.P. Conner, G.P. Manogharan, A.N. Martof, L.M. Rodomsky, C.M. Rodomsky, D.C. Jordan,J.W. Limperos, Making sense of 3-D printing: Creating a map of additive manufacturing products andservices, Additive Manufacturing 1–4(0) (2014) 64-76
32. Wang X, Xu S, Zhou S, Xu W, Leary M, Choong P, Qian M, Brandt M, Xie Y (2016) Topological design and additive manufacturing of porous metals for bone scaffolds and orthopedic implants: a review. Biomaterials 83:127–141
33. Murr LE (2016) Frontiers of 3D printing/additive manufacturing: from human organs to aircraft fabrication. J Mater Sci Technol 32: 987–995
34. Sing S, An J, Yeong W, Wiria F (2016) Laser and electron-beam powder-bed additive manufacturing of metallic implants: a review on processes, materials and designs. JOrthop Res 34(3):369–385
35. Yap C, Chua C, Dong Z, Liu Z, Zhang D, Loh L, Sing S (2015) Review of selective laser melting: materials and applications. Appl Phys Rev 2(4):041101
36. Tofail S, Koumoulos E, Bandyopadhyay A, Bose S, O'Donoghue L, Charitidis C (2018) Additive manufacturing: scientific and technological challenges, market uptake and opportunities. Mater Today 21(1):22–37
37. Atzeni E, Salmi A (2012) Economics of additive manufacturing for end-usable metal parts. Int J Adv Manuf Technol 62(9–12): 1147–1155
38. Schwab K (2017) The Fourth Industrial Revolution. Crown Business, New York, NY, USA
39. Wohlers Associates Inc, Wohlers report—3D printing and additive manufacturing state of the industry, in: Annual Worldwide Progress Report2016, Wohlers Associates Inc., Fort Collins, Colorado, 2016
40. R. L. Deuis; C. Subramanian" & J. M. Yellupb, Dry sliding Wear of Aluminium Composites-A Review,Composite and science and technology.57(4)(1997)415-435
41. Kempen K, Thijs L, Humbeeck JV, Kruth JP (2015) Processing AlSi10Mg by selective laser melting: parameter optimization and material characterization. Mater Sci Technol 31:917–923
42. Martin JH, Yahata BD, Hundley JM, Mayer JA, Schaedler TA, Pollock TM (2017) 3D printing of high-strengthaluminium alloys. Nature. 549:365–369
43. Jung JG, Ahn TY, Cho YH, Kim SH, Lee JM (2018) Synergistic effect of ultrasonic melt treatment and fast cooling on the refinement of primary Si in a hypereutectic Al–Si alloy. Acta Mater 144: 31–40
44. Jung JG, Lee SH, Cho YH, Yoon WH, Ahn TY, Ahn YS, Lee JM (2017) Effect of transition elements on the microstructure and tensile properties of Al–12Si alloy cast under ultrasonic melt treatment. J Alloys Compd 712:277–287
45. Reddappa H. N, Suresh K. R, Niranjan H. B, Satyanarayana K. G, Dry sliding friction and wear behavior of Aluminium/Beryl composites, International Journal of Applied Reseach,Dindigul,2(2) (2011)502-511.
46. Cáceres CH, Davidson CJ, Griffiths JR (1995) The deformation and fracture behavior of an Al-Si- Mg casting alloy. Mater Sci Eng A 197(1995):171–179
47. Kruth JP et al (2007) Consolidation phenomena in laser and powder-bed based layered manufacturing. CIRP Ann Manuf Technol 56(2):730–759
48. Kruth, J.P., et al.: Benchmarking of different SLS/SLM processes as rapid manufacturing techniques. In: International Conference on Polymers and Moulds Innovations (PMI), Gent, Belgium.(2005)1-7
49. Sercombe TB, Li X (2016) Selective laser melting of aluminium and aluminium metal matrix composites: review. Mater Technol 31(2):77–85
50. Mukherjee T, Wei HL, De A, DebRoy T (2018) Heat and fluid flow in additive manufacturing – Part II: Powder bed fusion of stainless steel, and titanium, nickel and aluminum base alloys. Comput Mater Sci 150:369–380
51. Dong-GyuAhn, Direct Metal Additive Manufacturing Processes and Their Sustainable Applications for Green Technology: A Review, international journal of precision engineering and manufacturing-green technology. 3 (2016)381-395
52. F. R. Kaschel, M. Celikin, D.P. Dowling,Effects of laser power on geometry, microstructure and echanical properties of printed Ti-6Al-4V parts, Journal of Materials Processing Technology.(278)(2020) 116539
53. Wang L, Dong C, Kong D, Man C, Liang J, Wang C, Li X (2019) *The Effect of Manufacturing Parameters on the Mechanical and Corrosion Behavior of Selective Laser Melted 15-5PH Stainless Steel. Steel Research International* 1900447
54. Hahn Choo, Kin-Ling Sham, John Bohling, Austin Ngo, Xianghui Xiao, Yang Ren, Philip J. Depond, Manyalibo J. Matthews, Elena Garlea,Effect of laser power on defect, texture, and microstructure of a laser powder bed fusion processed 316L stainless steel, Materials& Design.164(2019)107534
55. Reza Esmaeilizadeh, Ali Keshavarzkermani, Usman Ali, Behzad Behravesh, Ali Bonakdar, Hamid Jahed, Ehsan Toyserkani, On the effect of laser powder-bed fusion process parameters on quasi-static and fatigue behaviour of Hastelloy X: A microstructure/defect interaction study, Additive Manufacturing.38(2021) 101805
56. Pan Lu, Zhang Cheng-Lin, Wang Liang, Liu Tongand Li Xiao-Cheng, Research on mechanical properties and microstructure by selective laser melting of 316L stainless steel, Materials Research Express.6(12) (2019) 1265h7

57. AbanLarimian, Manigandan Kannan, Dariusz Grzesiak, Bandar AlMangour, Tushar Borkar,Effect of energy density and scanning strategy on densification, microstructure and mechanical properties of 316L stainless steel processed via selective laser melting, Materials Science and Engineering: A.770(2020)138455
58. Ilyas Hacısalihoğlu, FatihYıldiz, AyhanÇelik,The effects of build orientation and hatch spacing on mechanical properties of medical Ti–6Al–4V alloy manufactured by selective laser melting, Materials Science and Engineering: A .802(2021) 140649
59. Alexander Leicht, Camille Pauzon, Masoud Rashidi, Uta Klement, Lars Nyborg, Eduard Hryha,Effect of part thickness on the microstructure and tensile properties of 316L parts produced by laser powder bed fusion, Advances in Industrial and Manufacturing Engineering,.2(2021)100037
60. Gan L, Cheng Guo, Wenfeng Guo, Hongxing Lu, LinjuWen, Xiaogang Hu and Qiang Zhu, Influence of Selective Laser Melting Process Parameters on Densification Behavior, Surface Quality and Hardness of 18Ni300 Steel, *Key Engineering Materials,861(2020) 77-82*
61. Bhishek Mehta, Le Zhou, Thinh Huynh, Sharon Park, Holden Hyer, Shutao Song, Yuanli Bai, D. Devin Imholte, Nicolas E. Woolstenhulme, Daniel M. Wachs, YonghoSohn,Additive manufacturing and mechanical properties of the dense and crack free Zr-modified aluminum alloy 6061 fabricated by the laser-powder bed fusion, Additive Manufacturing..41 (2021) 101966
62. Zhiheng Hu, Yang Qi, Shubo Gao, XiaojiaNie, Hu Zhang, Haihong Zhu, XiaoyanZeng,Aging responses of an Al-Cu alloy fabricated by selective laser melting, Additive Manufacturing37 (2021) 101635
63. Cerri E, Ghio E, Bolelli G (2021) Effect of the Distance from Build Platform and Post-Heat Treatment of AlSi10Mg Alloy Manufactured by Single- and Multi-Laser Selective Laser Melting. *J of MateriEng and Perform*
64. Peidong He, Hui Kong, Qian Liu, Michael Ferry, Jamie J. Kruzic, XiaopengLi,Elevated temperature mechanical properties of TiCN reinforced AlSi10Mg fabricated by laser powder bed fusion additive manufacturing, Materials Science and Engineering: A.811(2021) 141025
65. Anton S. Konopatsky, Dmitry G. Kvashnin, Shakti Corthay, Ivan Boyarintsev, Konstantin L. Firestein, Anton Orekhov, Natalya Arkharova, Dmitry V. Golberg, Dmitry V. Shtansky, Microstructure evolution during AlSi10Mg molten alloy/BN microflake interactions in metal matrix composites obtained through 3D printing, Journal of Alloys and Compounds,Volume .859 (2021) 157765
66. Pelevin IA, Nalivaiko AY, Ozherelkov DY, Shinkaryov AS, Chernyshikhin SV, Arnautov AN, Zmanovsky SV, Gromov AA (2021) Selective Laser Melting of Al-Based Matrix Composites with Al_2O_3 Reinforcement: Features and Advantages. *Materials*. *14*:2648
67. Astm, Iso. "ASTM52900-15 standard terminology for additive manufacturing—general principles—terminology." *ASTM International, West Conshohocken, PA.* 3(4) (2015) 5.
68. ASTM F2792-12a: Standard Terminology for Additive Manufacturing Technologies,(2012)
69. Frazier WE (2014) Metal additive manufacturing: A review. J Mater Eng Perform 23:1917–1928
70. Herzog D, Seyda V, Wycisk E, Emmelmann C (2016) Additive manufacturing of metals. Acta Mater 117:371–392
71. Sames WJ, List FA, Pannala S, Dehoff RR, Babu SS (2016) The metallurgy and processing science of metal additive manufacturing. Int Mater Rev 61:315–360
72. Dutta B, Froes FH (2014) Additive manufacturing of titanium alloys. Adv Mater Process 172:18–23
73. Calignano F, Manfredi D, Ambrosio EP, Iuliano L, Fino P (2013) Influence of process parameters on surface roughness of aluminium parts produced by DMLS. Int J Adv Manuf Technol 67(9–12):2743–2751
74. G.P. Dinda, A.K. Dasgupta, J. Mazumder, Evolution of microstructure in laser deposited Al-11.28%Si alloy, Surf. Coat. Technol. 206 (2012) 2152–2160,
75. Dinda GP, Dasgupta AK, Bhattacharya S, Natu H, Dutta B, Mazumder J (2013) Microstructural characterization of laser-deposited Al 4047 alloy. Metall Mater Trans A Phys Metall Mater Sci 44:2233–2242
76. A. Singh, A. Ramakrishnan, G.P. Dinda, in: Direct laser metal deposition of eutectic Al-Si alloy for automotive applications, TMS 2017 146th Annual Meeting & Exhibition Supplemental Proceedings, 2017
77. F.A. Espan˜ a, V.K. Balla, A. Bandyopadhyay, Laser processing of bulk Al–12Si alloy: influence of microstructure on thermal properties, Philos. Mag. 91 (2011) 574–588
78. Yap CY, Chua CK, Dong ZL, Liu ZH, Zhang DQ, Loh LE, Sing SL (2015) Review of selective laser melting: materials and applications. Appl Phys Rev 2:041101
79. Wohlers T (2014) Wohlers Report : 3D Printing and Additive Manufacturing State of the Industry Annual Worldwide Progress Report. Fort Collins, WohlersAssociatesInc.
80. Kruth JP, Mercelis P, Froyen L, Rombouts M (2005) Binding mechanisms in selective laser sintering and selective laser melting. Rapid Prototyp J 11:25–36
81. Olakanmi EO, Cochrane RF, Dalgarno KW (2015) A review on selective laser sintering/ melting (SLS/SLM) of aluminium alloy powders: processing, microstructure, and properties. Prog Mater Sci 74:401–477
82. Gu DD, Meiners W, Wissenbach K, Poprawe R (2012) Laser additive manufacturing of metallic components: materials, processes and mechanisms. Int Mater Rev 57:133–164
83. https://www.eos.imaging.com
84. https://www.trumpf.com
85. Herzog D, Seyda V, Wycisk E, Emmelmann C (2016) Additive manufacturing of metals. Acta Mater 117:371–392
86. Aboulkhair NT, Everitt NM, Ashcroft I, et al. Reducing porosity in AlSi10Mg parts processed by selective laser melting. Additive Manufacturing .(1–4) (2014)77–86.
87. Aboulkhair NT, Maskery I, Tuck C, et al. Improving the fatigue behavior of a selectively laser melted aluminium alloy: influence of heat treatment and surface quality. Mater Des;104(2016) 174–82.
88. Martin JH, Yahata BD, Hundley JM, et al. 3D printing of high-strength aluminium alloys. Nature .549(7672)(2017)365.
89. Calignano F. Investigation of the accuracy and roughness in the laser powder bed fusion process. Virtual Phys Prototyping .13(2)(2018)97-104
90. Sing S, An J, Yeong W et al (2016) Laser and electron-beam powder-bed additive manufacturing of metallic implants: a review on processes, materials and designs. J Orthop Res 34(3):369–385
91. Yin, H. &Felicelli, S. D. Dendrite growth simulation during solidification in the LENS process. *Acta Materialia*58(4)((2010). 1455-1465.
92. Amano RS, Rohatgi PK (2011) Laser engineered net shaping process for SAE 4140 low alloy steel. *Mater Sci Eng A* 528(22-23): 6680–6693
93. Bian, L., Thompson, S. M. &Shamsaei, N.. Mechanical Properties and Micro structural Features of Direct Laser-Deposited Ti-6Al-4V.*Jom*67(3)(2015)629-638.
94. Gåård, A., Krakhmalev, P., and Bergström, J.. Microstructural characterization and wear behavior of (Fe,Ni)–TiC MMC prepared by DMLS. Journal of Alloys and Compounds, 421, (2016)166–171.

95. Jhabvala J et al (2010) On the effect of scanning strategies in the Selective Laser Melting process. Virtual and Physical Prototyping 5:99–109
96. Yasa E et al (2010) Charpy impact testing of metallic Selective Laser Melting parts. Virtual and Physical Prototyping 5:89–98
97. Bhattacharya S et al (2011) Micro structural evolution and mechanical, and corrosion property evaluation of Cu–30Ni alloy formed by Direct Metal Deposition process. J Alloys Compd 509:6364–6373
98. Delgado J, Ciurana J, Serenó L (2011) Comparison of forming manufacturing processes and Selective Laser Melting technology based on the mechanical properties of products. Virtual and Physical Prototyping 6:167–178
99. Yang T, Liu T, Liao W, MacDonald E, Wei H, Chen X, Jiang L (2019) The influence of process parameters on vertical surface roughness of the AlSi10Mg parts fabricated by selective laser melting. J Mater Process Technol 266:26–36
100. R. Lachmayer, Y. A. Zghair, C. Klose and F. Nürnberger, introducing selective laser melting to manufacture machine elements, international design conference - design .(2016) 831-842
101. T. G Spears,.A. Gold, In-procress sensing in selective laser melting (SLM) additive manufacturing, Integrating materials and Manufacturing Innovation .5 (2016) 16-40
102. H. Asgari, C. Baxter, K. Hosseinkhani, M. Mohammadi, On microstructure and mechanical properties of additively manufactured AlSi10Mg 200C usingrecycled powder, Mater. Sci. Eng.: A 707 (2017) 148–158.
103. E.O. Olakanmi, R.F. Cochrane, K.W. Dalgarno, A review on selective laser sintering/melting (SLS/SLM) of aluminium alloy powders: processing,microstructure, and properties, Prog Mater Sci 74 (2015) 401–477.
104. Bin Anwar A, Cuong Pham Q (2017) Selective laser melting of AlSi10Mg: effects of scan direction, part placement and inert gas flow velocity on tensile strength. J Mater Process Technol 240: 388–396
105. Trevisan F et al (2017) On the selective laser melting (SLM) of the AlSi10Mg alloy: process, microstructure, and mechanical properties. Materials 10:76
106. Krishnan M et al (2014) On the effect of process parameters on properties ofAlSi10Mg parts produced by DMLS. Rapid Prototyp J 20:449–458
107. Kempen K, Thijs L, Van Humbeeck J, Kruth J-P (2015) Processing AlSi10Mg by selective laser melting: parameter optimization and material characterization. Mater Sci Technol 31: 917–923
108. Read N, Wang W, Essa K, Attallah MM (2015) Selective laser melting of AlSi10Mgalloy: process optimization and mechanical properties development. Mater.Des. 65:417–424
109. Arfan Majeed, Yingfeng Zhang, JingxiangLv, Tao Peng, Zahid Atta, Altaf Ahmed, Investigation of T4 and T6 heat treatment influences on relative density and porosity of AlSi10Mg alloy components manufactured by SLM,Computers& Industrial Engineering.139(2020) 106194 .
110. Yasa, E., Kruth, J.-P.: Application of laser re-melting on selective laser melting parts. Additive .Prod. Eng. Manag. 6(4) (2011) 259–270
111. Monroy K, Delgado J, Ciurana J (2013) Study of the pore formation on CoCrMo alloys by selective laser melting manufacturing process. Procedia Eng 63:361–369
112. Louvis E, Fox P, Sutcliffe CJ (2011) Selective laser melting of aluminium components. Journal ofMaterials Processing Technology 211:275–284
113. K. Kempen, L. Thijs, E. Yasa, M. Badrossamay, W; Verheecke, J.P. Kruth, Process optimization and micro structural analysis for selective laser melting of AlSi10Mg, International Solid Freeform fabrication Symposium 22 (2011) 484-449
114. Quintino L, Miranda R, Dilthey U, Iordachescu D, Banasik M, Stano S (2012) Laser Welding of Structural Aluminium. Adv Struct Mater 8:33–57
115. Arata Y, Miyamoto I (1972) Some fundamental properties of high power laser beam as a heat source (report 2) – CO2 laser absorption characteristics of metal. Transactions of the Japan Welding Society 3:152–162
116. ASM specialty handbook, Aluminium and aluminium alloys, sixth printing, (2007)720
117. Saket Thapliyal, MageshwariKomarasamy, Shivakant Shukla, Le Zhou, Holden Hyer, Sharon Park, Yongho Sohn, Rajiv S. Mishra, An integrated computational materials engineering-anchored closed-loop method for design of aluminum alloys for additive manufacturing, Materialia,9(2020)100574.
118. Kumar S (2014) Selective laser sintering/melting. In: Hashmi S (ed) Comprehensive Materials Processing. Elsevier, Amsterdam, pp 93–133
119. Emmelmann C, Sander P, Kranz J, Wysick E (2011) Laser additive manufacturing and bionics. Phys Procedia 12:364–368
120. Gibson I, Rosen DW, Stucker B (2015) Additive Manufacturing Technologies, Rapid Prototyping to Direct Digital Manufacturing. Springer, Verlag, New York 2015
121. Ardila, L.C., Garciandia, F., González-Díaz, J.B., Álvarez, P., Echeverria, A., Petite,M.M., Deffley, R., Ochoaa, J.,. Effect of IN718 recycled powder reuse on properties of parts manufactured by means of selective laser melting. Phys Procedia 56 (2014) 99–107.
122. Lishi Jiao , Zhong Yang Chua , Seung Ki Moon , Jie Song , Guijun Bi and Hongyu Zheng, Femtosecond Laser Produced Hydrophobic Hierarchical Structures on Additive Manufacturing Parts, Nonmaterial's.8(8)(2018)601
123. Khaing MW, Fuh JYH, Lu L (2001) Direct Metal Laser Sintering for rapid tooling: Processing andcharacterization of EOS parts. J Mater Process Technol 113:269–272
124. https://www.eos.info/en
125. Wohlers, T. T. and Caffrey, T., Wohlers Report : 3D Printing and Additive Manufacturing State of the Industry Annual Worldwide Progress Report," Wohlers Associates.(2015).
126. http://www.eos.info/systems_solutions/metal
127. Kruth, J. P., Mercelis, P., Froyen, L., and Rombouts, M., Binding Mechanisms in Selective Laser Sintering and Selective Laser Melting.11(1)(2005)26-36
128. Aboulkhair NT, Maskery I, Tuck C, Ashcroft I, Everitt NM (2016) The microstructure and mechanical properties of selectively laser melted AlSi10Mg: the effect of a conventional T6-like heat treatment. Mater Sci Eng A 66:139–146
129. Wohlers, T. T. and Caffrey, T., Wohlers Report : 3D Printing and Additive Manufacturing State of the Industry Annual Worldwide Progress Report," Wohlers Associates.(2015).
130. Strano G, Hao L, Everson RM, Evans KE (2013) Surface roughness analysis, modeling and prediction in selective laser melting. J Mater Process Technol **213**(4):589–597
131. Atzeni, E., Salmi, A., Incontro, M., A DoE approach for evaluating the quality of self supporting faces in DMLS, in 4th International Conference on Additive Technologies (iCAT 2012).(2012)
132. Calignano F, Manfredi D, Ambrosio EP, Iuliano L, Fino P (**2013**) Influence of process parameters on surface roughness of aluminum parts produced by DMLS. *Int J Adv Manuf Technol* **67**:**2743**–**2751**
133. https://www.custompartnet.com/
134. Herzog D, Seyda V, Wycisk E, Emmelmann C (2016) Additive manufacturing of metals. Acta Mater 117(2016):371–392
135. Lewandowski JJ, Seifi M (2016). Annu Rev Mater Res 46:151–186

136. Everton SK, Hirsch M, Stravroulakis P, Leach RK, Clare AT (2016) Review of in-situ process monitoring and in-situ metrology for metal additive manufacturing. Mater Des 95:431–445
137. DebRoy T, Wei HL, Zuback JS, Mukherjee T, Elmer JW, Milewski JO, Beese AM, Wilson-Heid A, De A, Zhang W (2018) Additive manufacturing of metallic components – Process, structure and properties. Prog Mater Sci 92:112–224
138. Tapia, G.; Elwany, A. A review on process monitoring and control in metal-based additive manufacturing's. Manuf. Sci. E .136(2014) 060801.
139. Mower, T.M.; Long, M.J. Mechanical behavior of additive manufactured, powder-bed laser-fused materials. Mater. Sci. Eng. A .651(2016) 198–213
140. Kimura T, Nakamoto T (2017) Thermal and mechanical properties of commercial-purity aluminium fabricated using selective laser melting. Mater Trans 58:799–805
141. Herzog D, Seyda V, Wycisk E, Emmelmann C (2016) Additive manufacturingof metals. Acta Mater 157:371–392
142. Wohlers Report, Additive Manufacturing and 3D Printing State on the industry, Wohlers Associates, Fort Collins, Colorado, ICED15.12(2013)
143. Petroušek P, Bidulská J, Bidulský R, Kocisko R, Fedorikova A, Hudak R, Rajtukova V, Zivcak J (2017) Mechanical properties and porosity of Ti-6Al-4V alloy prepared by AM technology. MM Science Journal:1752–1755
144. AlicaFedorikova, Radovan Hudak,,Jozefzivcak, Robert bidulsky, PatrikPetrousek, Jana Bidulska1,Robert Kocisko1,Viktoria Rajtukova, Mechanical properties of powder cocrw-alloy prepared by am technology. ,MM Science Journal, (2016)1586-1589
145. Hamidi Nasab M, Gastaldi D, Lecis NF, Vedani M (2018) On morphological surface features of the parts printed by selective laser melting (SLM). Addit Manuf 24:373–377
146. Yadroitsev I, Smurov I (2011) Surface morphology in selective laser melting of metal powders, in: Physics. Procedia.
147. Townsend A, Senin N, Blunt L, Leach RK, Taylor JS (2016) Surface texture metrology for metal additive manufacturing: a review. Precis Eng 46:34–47
148. J.S. Taylor, Physical processes linking input parameters and surface morphology in additivemanufacturing, in: Proc. - ASPE 2015 Spring Top. Meet. Achiev. Precis. Toler.Addit. Manuf.(2015) 70-71.
149. L. zhi Wang, S. Wang, J. jiao Wu, Experimental investigation on densification behavior and surface roughness of AlSi10Mg powders produced by selective laser melting, Opt. Laser Technol. 96 (2017) 88–96.
150. Mumtaz K, Hopkinson N (2009) Top surface and side roughness of Inconel 625 parts processed using selective laser melting. Rapid Prototyp J 15:96–103
151. Strano G, Hao L, Everson RM, Evans KE (2013) Surface roughness analysis, modeling and prediction in selective laser melting. J Mater Process Technol 213:589–597
152. J.C. Fox, S.P. Moylan, B.M. Lane, Effect of Process Parameters on the Surface Roughness of Overhanging Structures in Laser Powder Bed Fusion Additive Manufacturing, in: Procedia.45(2016)131-134
153. Manfredi D et al (2014) Additive manufacturing of Al alloys and Aluminium Matrix Composites (AMCs), in: Light Metal Alloys Applications, edited by W. A Monteiro
154. Kruth JP, Mercelis P, Van Vaerenbergh J, Froyen L, Rombouts M (2005) Binding mechanisms in selective laser sintering and selective laser melting. Rapid Prototyp J 11:26–36
155. Niu HJ, Chang ITH (2000) Selective laser sintering of gas atomized M2 high speed steel powder. J Mater Sci 35:31–38
156. Manfredi D et al (2013) From powders to dense metal parts: characterization of commercial AlSiMg alloy processed through direct metal laser sintering. Materials 6:856–869
157. https://www.bintoa.com/powder-bed-fusion/
158. Buchbinder D, Schleifenbaum H, Heidrich S, Meiners W, Bültmann J (2011) High power Selective Laser Melting (HP SLM) of aluminum parts. Phys Procedia 12:271–280
159. Read N, Wang W, Essa K, Attallah MM. Selective laser melting of AlSi10Mg alloy: process optimization and mechanical properties development. Mater Des .65(2015)417-424.
160. Zhang J, Song B, Wei Q, Bourell D, Shi Y (2019) A review of selective laser melting of aluminium alloys: processing, microstructure, property and developing trends. J Mater Sci Technol 35:270e284
161. R. Li, M. Wang, T. Yuan, B. Song, C. Chen, K. Zhou, P. Cao, Selective laser melting of a novel Sc and Zr modified Al-6.2 Mg alloy: processing, microstructure, and properties, Powder Technol. 319 (2017) 117e128.
162. Wang M, Song B, Wei Q, Zhang Y, Shi Y (2019) Effects of annealing on the microstructure and mechanical properties of selective laser melted AlSi7Mg alloy. Mater Sci Eng A 739:463e472
163. R. Li, M. Wang, T. Yuan, B. Song, C. Chen, K. Zhou, P. Cao, Selective laser melting of a novel Sc and Zr modified Al-6.2 Mg alloy: Processing ,microstructure, and properties, Powder Technol. 319 (2017) 117-128.
164. Rao H, Giet S, Yang K, Wu X, Davies CHJ (2016) The influence of processing parameters on aluminium alloy A357 manufactured by Selective Laser Melting. Mater Des 109:334–346
165. Bartkowiak K, Ullrich S, Frick T, Schmidt M (2011) New Developments of Laser Processing Aluminium Alloys via Additive Manufacturing Technique. Phys Procedia 12:393–401
166. Buchbinder D, Schleifenbaum H, Heidrich S, Meiners W, Bültmann J (2011) High power selective laser melting (HP SLM) of aluminum parts. Phys Procedia 12:271–278
167. Li Y, Gu D (2014) Parametric analysis of thermal behavior during selective laser melting additive manufacturing of aluminum alloy powder. Mater Des 63:856–867
168. H. Zhang, H. Zhu, X Nie, J Yin, Z Hu, X Zeng, Effect of Zirconium addition on crack, microstructure and mechanical behavior of selective laser melted Al-Cu-Mg alloy, Script Materialia134 (2017) 6-10
169. Aboulkhair NT, Maskery I, Tuck C, Ashcroft I, Everitt NM (2016) On the formation of AlSi10Mg single tracks and layers in selective laser melting: Microstructure and nano-mechanical properties. J Mater Process Technol 230:88–98
170. Louvis E, Fox P, Sutcliffe CJ (2011) Selective laser melting of aluminium components. J Process Technol 211:275–284
171. Loto CA (2016) Electroless nickel plating – a review. Silicon. 8: 177–186
172. Tolochko NK, Laoui T, Khlopkov YV, Mozzharov SE, Titov VI, Ignatiev MB (2000) Absorptance of powder materials suitable for laser sintering. Rapid Prototyp J 6:155–160
173. Fischer P, Romano V, Weber HP, Karapatis NP, Boillat E, Glardon R (2003) Sintering of commercially pure titanium powder with a Nd:YAG laser source. Acta Mater 51:1651–1662
174. Lekatou AG, Sfikas AK, Karantzalis AE (2017) The influence of the fabrication route on the microstructure and surface degradation properties of Al reinforced by Al9Co2. Mater Chem Phys 200:33–49
175. Huber F, Papke T, Scheitler C, Hanrieder L, Merklein M, Schmidt M (2018) In situ Formation of a Meta stable β-Ti Alloy by Laser Powder Bed Fusion(L-PBF) of Vanadium and Iron Modified Ti-6Al-4V. Metals. 8:1067
176. Zhou W, Dong M, Zhou Z, Sun X, Kikuchi K, Nomura N, Kawasaki A (2019) In situ formation of uniformly dispersed Al4C3 nano rods during additive manufacturing of grapheme oxide/Al mixed powders. Carbon. 141:67–75

177. Zhou W, Sun X, Kikuchi K, Nomura N, Yoshimi K, Kawasaki A (2018) In situ synthesized Tic/Mo-based composites via laser powder bed fusion. Mater Des 146:116–124
178. Yadroitsev I, Krakhmalev P, Yadroitsava I (2017) Titanium alloys manufactured by in situ alloying during laser powder bed fusion. JOM. 69:2725–2730
179. Geng K, Yang Y, Li S, Misra RDK, Zhu Q, Enabling high-performance 3D printing of Al powder by decorating with high laser absorbing Co phase, Additive Manufacturing .32(2020)101012
180. Galy C, Le Guen E, Lacoste E, Arvieu C (2018) Main defects observed in aluminum alloy parts produced by SLM: from causes to consequences. Additive Manufacturing 22:165–175
181. Wong M, Tsopanos S, Sutcliffe CJ, Owen I (2017) Selective laser melting of heat transfer devices. Rapid Prototyp J 13:291–297
182. Takahiro. Kimura, Takayuki Nakamoto, Masataka Mizuno and Hideki Araki, "Effect of silicon content on densification, mechanical and thermal properties of Al-xSi binary alloys fabricated using selective laser meltin, *Materials Science & Engineering A.682(13) (2017)593-602*
183. Osório WR, Goulart PR, Garcia A (2008) Effect of silicon content on microstructure and electrochemical behavior of hypoeutectic Al-Si alloys. Mater Lett 62(2008):365–369
184. Ponnusamy MSH, Ruan D, Palanisamy S, Rahman RA, Kariem RMA (2018) High strain rate behaviour at high temperature of AlSi12 parts produced by selective laser melting. IOP Conf. Series: Materials Science Eng 377:012167
185. Rashid R, Masood SH, Ruan D, Palanisamy S, Rahman Rashid RA, Elambasseril J, Brandt M (2018) Effect of energy per layer on the anisotropy of selective laser melted AlSi12 aluminium alloy. Additive Manufacturing 22:426–439
186. Vora P, Mumtaz K, Todd I, Hopkinson N (2015) AlSi12 in-situ alloy formation and residual stress reduction using anchorless selective laser melting. Additive Manufacturing 9:7–12
187. Wang X, Zhang L, Fang M, Sercombe TB (2014) The effect of atmosphere on the structure and properties of a selective laser melted Al–12Si alloy. Mat Sci and Engg: A 597(12):370–375
188. Siddique S, Imran M, Wycisk E, Emmelmann C, Walther F (2015) Influence of process-induced microstructure and imperfections on mechanical properties of AlSi12 processed by selective laser melting. J Mat Processing Tech 221:205–213
189. Siddique S, Imran M, Walther F (2017) Very high cycle fatigue and fatigue crack propagation behavior of selective laser melted AlSi12 alloy. Int J Fatigue 94:246–254
190. Prashanth K, Scudino S, Klauss H, Surreddi KB, Löber L, Wang Z, Chaubey A, Kühn U, Eckert J (2014) Microstructure and mechanical properties of Al–12Si produced by selective laser melting: Effect of heat treatment. Mat Sci Engg: A 590:153–160
191. Li X, Wang X, Saunders M, Suvorova A, Zhang L, Liu Y, Fang M, Huang Z, Sercombe TB (2015) A selective laser melting and solution heat treatment refined Al–12Si alloy with a controllable ultrafine eutectic microstructure and 25% tensile ductility. Acta Mater 95:74–82
192. Fefelov AS, Merkushev AG, Chikova OA (2017) Microstructure and mechanical properties of Al-12Si produced by selective laser melting. IOP Conf Series: Earth and Environmental Science 87: 092011
193. Jyoti S, Prashanth KG, Scudino S, Eckert J, Prakash O, Ramamurty U (2016) Simultaneous enhancements of strength and toughness in an Al-12Si alloy synthesized using selective laser melting. Acta Mater 115:285–e294
194. Louvis E, Fox P, Sutcliffe CJ (2011) Selective laser melting of aluminium components. J Mater Process Technol 211:275–284
195. Olakanmi EO, Cochrane RF, Dalgarno KW (2011) Densification mechanism and microstructural evolution in selective laser sintering of Al–12Si powders. J Mater Process Technol 217: 113–121
196. Li XP, O'Donnell KM, Sercombe TB (2016) Selective laser melting of Al-12Si alloy: Enhanced densification viapowder drying. Additive Manufacturing 10:10–14
197. Kang N, Coddet P, Linliao H, Baur T, Coddet C (2016) Wear behavior and microstructure of hypereutectic Al-Si alloys prepared by Selective laser melting. Appl Surf Sci 378:142–149
198. Siddique S, Imran M, Rauer M, Kaloudis M, Wycisk E (2015) Computed tomography for characterization of fatigue performance of selective laser melted parts. Mater Des 83:661–669
199. Prashanth KG, Scudino S, Eckert J (2016) Tensile properties of Al-12Si fabricated via selective laser melting (SLM) at different temperatures. Technologies 4(4):38
200. Pan M, Prashanth KG, Scudino S, Jia Y, Wang H, Zou C, Wei Z, Eckert J (2014) Influence of annealing on mechanical properties of Al-20Si processed by selective laser melting. Metal 4:*28–36*
201. Dörfert R, Stoll C, Freiße H, Seefeld T, Vollertsen F (2017) Influence of the process on surface roughness of 3D-printed aluminum alloy AlSi40 parts. International Journal of Latest Research in Engineering and Technology 3(10):35–41
202. Mueller M, Riede M, Eberle S, Reutlinger A, Brandão AD, Pambaguian L, Seidel A, López E, Brueckner F, Beyer E, Leyens C (2019) Micro structural, mechanical, and thermophysical characterization of hypereutectic AlSi40 fabricated by selective laser melting. J Laser Appl 31:022321
203. Hanemann T, Carter LN, Habschied M, Adkins NJE, Attallah MM, Heilmaier M (2019) In-situ alloying of AlSi10MgþSi using Selective Laser Melting to control the coefficient of thermal expansion. J Alloys Compd 795:8e18
204. ASM Handbook (1990) Volume 2, Properties and Selection: Non ferrous Alloys and Special-Purpose Materials, ASM International, Materials Park, OH
205. González R, González A, Talamantes-Silva J, Valtierra S, Mercado-Solís RD, Garza-Montes-de-Oca NF, Colás R (2013) Fatigue of an aluminium cast alloy used in the manufacture of automotive engine blocks. Int J Fatigue 54(0):118–126
206. Zebala W, Kowalczyk R, Matras A (2015) Analysis and optimization of sintered carbides turning with PCD tools. Procedia Eng 100:283–290
207. Read N, Wang W, Essa K, Attallah MM (2015) Selective laser melting of AlSi10Mg alloy: Process optimisation and mechanical properties development. Mater Des 65:417–424
208. Godino Martinez M (2013) AlSi10Mg parts produced by selective laser melting (SLM) (masters). Universidad Carlos III de Madrid
209. Santos MC, Machado AR, Sales WF, Barrozo M, Ezugwu EO (2016) Machining of aluminium: a review. Int J Adv Manuf Technol 86:3067–3080
210. Buchbinder D, Schleifenbaum H, Heidrich S, Meiners W, Bültmann J (2011) High power Selective Laser Melting (HP SLM) of aluminum parts. Phys Procedia 12:271–280
211. Kempen K, Thijs L, Van Humbeek J, Kruth J-P (2012) Mechanical properties of AlSi10Mg produced by selective laser melting. Phys Procedia 39:439–446
212. Hitzler L, Janousch C, Schanz J, Merkel M, Heine B, Mack F et al (2017) Direction and location dependency of selective laser melted AlSi10Mg specimens. J Mater Process Technol 243:48–61
213. Brandl E, Heckenberger U, Holzinger V, Buchbinder D (2012) Additive manufactured AlSi10Mg samples using Selective Laser Melting (SLM): microstructure, high cycle fatigue, and fracture behaviour. Mater Des 34:159–169
214. Maskery I, Aboulkhair NT, Tuck C, Wildman RD, Ashcroft IA, Everitt NM, et al. .(2015) Fatigue performance enhancement of selectively laser melted aluminium alloy byheat treatment. In: Twenty-sixth annual international solid freeform fabrication

(SFF) symposium – an additive manufacturing conference, Texas, U.S.A. 1017-1026
215. Tang M, Chris PP (2017) Oxides, porosity and fatigue performance of AlSi10Mg parts produced by selective laser melting. Int J Fatigue 94:194–201
216. Aboulkhair NT, Maskery I, Tuck C, Ashcroft I, Everitt NM (2016) Improving the fatigue behaviour of a selectively laser melted aluminium alloy: influence of heat treatment and surface quality. Mater Des 104:174–182
217. Mower TM, Long MJ (2016) Mechanical behavior of additive manufactured, powder-bed laser-fused materials. Mater Sci Eng A 651:198–213
218. Olakanmi EO, Cochrane RF, Dalgarno KW (2015) A review on selective laser sintering/ melting (SLS/SLM) of aluminium alloy powders: processing, microstructure, and properties. Prog Mater Sci 74:401–477
219. Gu DD, Meiners W, Wissenbach K, Poprawe R (2012) Laser additive manufacturing of metallic components: materials, processes and mechanisms. Int Mater Rev 57:133–164
220. Li W, Li S, Liu J, Zhang A, Zhou Y, Wei Q, Yan C, Shi Y (2016) Effect of heat treatment on AlSi10Mg alloy fabricated by selective laser melting: microstructure evolution, mechanical properties and fracture mechanism. Mater Sci Eng A 663:116–125
221. Rosenthal I, Stern A, Frage N (2017) Strain rate sensitivity and fracture mechanismof AlSi10Mg parts produced by selective laser melting. Mater Sci Eng A 682:509–517
222. Asgari H, Odeshi A, Hosseinkhani K, Mohammadi M (2018) On dynamicmechanical behavior of additively manufactured AlSi10Mg 200C. Mater Lett 211:187–190
223. Zhang P, Li Z, Liu B, Ding W, Peng L (2016) Improved tensile properties of a newaluminum alloy for high pressure die casting. Mater Sci Eng A 651:376–390
224. Read N, Wang W, Essa K, Attallah M (2015) Selective laser melting of AlSi10Mg alloy: process optimisation and mechanical properties development. Mater Des 65:417–424
225. Krishnan M, Atzeni E, Canali R, Calignano F, Manfredi D, Ambrosio E, Iuliano L (2014) On the effect of process parameters on properties of AlSi10Mg partsproduced by DMLS. Rapid Prototyp J 20(6):449–458
226. Kempen K, Thijs L, Humbeeck J, Kruth J-P (2015) Processing AlSi10Mg by selective laser melting: parameter optimisation and material characterisation. Mater SciTechnol 31(8):917–923
227. Rosenthal I, Stern A, Frage N (2017) Strain rate sensitivity and fracture mechanism of AlSi10Mg parts produced by Selective Laser Melting. Mater Sci Eng A 682:509–517
228. Carter LN, Martin C, Withers PJ et al (2014) The influence of the laser scan strategy on grain structure and cracking behaviour in SLM powder-bed fabricated nickel superalloy. J Alloys Compd 615(2):338–347
229. Salmi A, Atzeni E (2017) History of residual stresses during the production phases of AlSi10Mg parts processed by powder bed additive manufacturing technology. Virtual Phys Prototyping 12(2):153–160
230. Zhu Y, Ding Z, Wang L et al (2018) Investigation of performance and residual stress generation of AlSi10Mg processed by selective laser melting. Adv Mater Sci Eng:7814039
231. Thijs L, Kempen K, Kruth J-P, Humbeeck JV (2013) Fine-structured aluminium products with controllable texture by selective laser melting of pre-alloyed AlSi10Mgpowder. Acta Mater 61:1809–1819
232. Lu L, Nogita K, Dahle AK (2005) Combining Sr and Na additions in hypoeutectic Al-Si foundry alloys. Mater Sci Eng A 399:244–253
233. Karakösea E, Keskin M (2009) Effect of solidification rate on the microstructure and microhardness of a melt-spun Al-8Si-1Sb alloy. J Alloys Compd 479:230–236
234. Sames W, List F, Pannala S, Dehoff R (2016) Metallurgy and processing science of metaladditive manufacturing. Int Mater Rev 61(5):315–360
235. Weingarten C, Buchbinder D, Pirch N, Meiners W, Wissenbach K, Poprawe R (2015) Formation and reduction of hydrogen porosity during selective laser melting ofAlSi10Mg. J Mater Process Technol 221:112–120
236. Aboulkhair NT, Everitt NM, Ashcroft I, Tuck C (2014) Reducing porosity inAlSi10Mg parts processed by selective laser melting. Addit Manuf 4:77–86
237. Weingarten C et al (2015) Formation and reduction of hydrogen porosity duringselective laser melting of AlSi10Mg. J Mater Process Technol 221:112–120
238. Aboulkhair NT, Everitt NM, Ashcroft I et al (2014) Reducing porosity in AlSi10Mg parts processed by selective laser melting. AdditManuf 1–4:77–86
239. Plessis AD, Yadroitsev I, Yadroitsava I et al (2018) X-ray microcomputed tomography in additive manufacturing: a review of the current technology and applications. 3D Print AdditManuf 5(3):227–247
240. Xu Z, Liu A, Wang X (2021) Fatigue performance and crack propagation behavior of selective laser melted AlSi10Mg in 0°, 15°, 45° and 90° building directions. Mater Sci Eng A 812:141141
241. Brandl E, Heckenberger U, Holzinger V, Buchbinder D (2012) Additivemanufactured AlSi10Mg samples using selective laser melting (SLM):microstructure, high cycle fatigue, and fracture behavior. Mater Des 34:159–169
242. Tang M, Pistorius PC (2017) Oxides, porosity and fatigue performance of AlSi10Mg parts produced by selective laser melting. Int J Fatigue 94:192–201
243. Aboulkhair NT, Everitt NM, Ashcroft I, et al., Reducing porosity in AlSi10Mg parts processed by selective laser melting. AdditManuf .1–4 (2014) 77–86.
244. Brandl E, Heckenberger U, Holzinger V, Buchbinder D. Additive manufactured AlSi10Mg samples using Selective Laser Melting (SLM): microstructure, high cyclefatigue, and fracture behaviour. Mater Des .34 (2012) 159–69.\
245. Tang M, Pistorius P Chris. Oxides, porosity and fatigue performance of AlSi10Mg parts produced by selective laser melting. Int J Fatigue 94 (2017) 192–201
246. A. Barari, H.A. Kishawy, F. Kaji, M.A. Elbestawi, On the surface quality of additive manufactured parts, Int. J. Adv. Manuf. Technol. 89 (2017)1969-1974.
247. Mohammadi M, Asgari H (2018) Achieving low surface roughness AlSi10Mg_200C parts using direct metal laser sintering. Addit Manuf 20:23–32
248. Leon A, Aghion E (2017) Effect of surface roughness on corrosion fatigue performance of AlSi10Mg alloy produced by Selective Laser Melting (SLM). Mater Charact 131:229–237
249. Uzan NE, Shneck R, Yeheskel O (2017) Frage N, Fatigue of AlSi10Mg specimens fabricated byadditive manufacturing selective laser melting (AM-SLM). Mater Sci Eng A 704:229–237
250. Günther, J., Leuders, S., Koppa, P., Tröster, T., Henkel, S., Biermann, H., Niendorf, T.,2018. On the effect of internal channels and surface roughness on the high-cycle fatigue performance of Ti-6Al-4V processed by SLM. Mater. Des. 143 (2018) 1-11
251. M. Jamshidinia, F. Kong, R. Kovacevic, The numerical modeling of fatigueproperties of a bio-compatible dental implant produced by electron beammelting (EBM), in: In Proceeding of the Twenty Forth Annual InternationalSolid Freeform Fabrication Symposium.(2013) 791-804
252. Stephens RI, Fatemi A, Stephens RR, Fuchs HO (2000) Metal Fatigue inEngineering. John Wiley & Sons
253. Zou Y et al (2017) The intergranular corrosion behavior of 6000-series alloys withdifferent Mg/Si and Cu content. Appl Surf Sci 405:489–496

254. Li T, Li XG, Dong CF, Cheng YF (2010) Characterization of atmospheric corrosionof 2A12 aluminum alloy in tropical marine environment. J Mater EngPerform 19:591–598
255. Molland AF, Turnock SR, Hudson DA (2017) Ship Resistance and Propulsion. Cambridge University Press
256. Wohlers, Wohlers Report 2014 - 3D Printing and Additive Manufacturing State of theIndustry Annual Worldwide Progress Report (2016).
257. Strano, G., Hao, L., Everson, R.M., Evans, K.E.., Surface roughness analysis, modellingand prediction in selective laser melting. Journal of Materials Processing Technology,.**213**(4) (2013) 589-597.
258. Bañón c., Raspall f. Additive Manufacturing Technologies for Architecture. In: 3D Printing Architecture. SpringerBriefs in Architectural Design and Technology. Springer, Singapore.(2021) 13-20.
259. Tian Y, Tomus D, Rometsch P, Wu X (2017) Influences of processing parameters on surface roughness of Hastelloy X produced by selective laser melting. Addit Manuf 13:103–112
260. Calignano F, Manfredi D, Ambrosio EP, Iuliano L, Fino P (2013) Influence of processparameters on surface roughness of aluminum parts produced by DMLS. InternationalJournal of Advanced Manufacturing Technology **67**(9-12):2743–2751
261. Gebhardt, A., Hötter, J.-S., Ziebura, D.: Impact of SLM build parameters on the surface quality. RTejournal - Forum für Rapid Technologie .11(2014)
262. Calignano F et al (2013) Influence of process parameters on surface roughness of aluminum parts produced by DMLS. Int J Adv Manuf Technol 67(9–12):2743–2751
263. Tian Y, Tomus D, Rometsch P, Wu X (2017) Influences of processing parameters on surface roughness of Hastelloy X produced by selective laser melting. Addit.Manuf. 13:103–112
264. Nguyen QB, Luu DN, Nai SML, Zhu Z, Chen Z, Wei J (2018) The role of powder layer thickness on the quality of SLM printed parts. Arch Civil Mech Eng 18:948–955
265. Calignano F (2018) Investigation of the accuracy and roughness in the laser powder bed fusion process. Virtual Phys Prototyp 13:97–104
266. Atzeni, E., Salmi, A., Incontro, M., Study on unsupported over hangs of AlSi10Mg parts. A DoE approach for evaluating the quality of selfsupporting faces in DMLS, in 4th International Conference on Additive Technologies (iCAT2012), D. International, Editor. 2012: Maribor, Slovenia
267. P.Ferro, R,meneghello, S.M.J.Razavi,F.Berto, and G.Savio,, Porasity inducing process parameters in selective laser melted AlSi10Mg AlloyPhysical meso mechanics, 23 (2020) 256-262
268. Ahmed A, Majeed A, Atta Z, Jia G (2019) Dimensional Quality and Distortion Analysis of Thin-Walled Alloy Parts of AlSi10Mg Manufactured by Selective Laser Melting. Journal of Manufacturing and Materials Processing 3(2):5
269. Xiaochuan Zhang , Jinwu Kang ,*, Yiming Rong , Pengyue Wu and Tao Feng ," Effect of Scanning Routes on the Stress and Deformation of Overhang Structures Fabricated by SLM, Materials.12(1) (2019) 47
270. Ahmed H. Maamoun, Yi F. Xue1, Mohamed A. Elbestawi 1, Stephen C. Veldhuis,"Effect of SLM process parameters on the quality of Al Alloy parts; Part I: powder characterization, density, surface roughness, and dimensional 2 accuracy"Peer-reviewed version available at Materials .11(2018)2343
271. Tao Yang, Tingting Liu, Wenhe Liao, Eric MacDonald, Huiliang Wei, Xiangyuan Chen, LiyiJiang,"The Influence of Process Parameters on Vertical Surface Roughness of the AlSi10Mg Parts Fabricated by Selective Laser Melting", J Mater Process Technol266 (2019) 26-36
272. S.A. Jawade , Rashmi.S. Joshi, S.B. Desai," Comparative study of mechanical properties of additively manufactured aluminum alloy", Materials Today: Proceedings ,2020.
273. NaorEladUzana,, Barak Ratzker, Peri Landau, Sergey Kalabukhov, Nachum Frage," Compressive creep of AlSi10Mg parts produced by selective laser melting additive manufacturing technology, Additive Manufacturing 29 (2019) 100788
274. .P. Lam, D.Q. Zhang, Z.H. Liu & C.K. Chua (2015): Phase analysis and microstructure characterisation of AlSi10Mg parts produced by Selective Laser Melting, Virtual and Physical Prototyping, virtual and physical prototyping.10(4) (2015) 207-215
275. Z. Dong, Y. Liu, Q. Zhang, J. Ge, S. Ji, W. Li, J. Liang, "Microstructural heterogeneity of AlSi10Mg alloy lattice structures fabricated by selective laser melting: Phenomena and mechanism", *Journal of Alloys and Compounds* .833(2020) 155071.
276. Hadadzadeh A, Amirkhiz BS, Shakerin S, Kelly J, Li J, Mohammadi M, Microstructural investigation and mechanical behavior of a two-material component fabricated through selective laser melting of AlSi104Mg on an Al-Cu-Ni-Fe-Mg cast alloy substrate, *Additive Manufacturing* .31 (2020)100937
277. K. Kamarudin1,, M.S. Wahab, Z. Shayfull, Aqeel Ahmed , and A.A. Raus," Dimensional Accuracy and Surface Roughness Analysis for AlSi10Mg Produced by Selective Laser Melting (SLM), MATEC Web of Conferences .7(2016) 01077
278. Ming Tang, P. Chris Pistorius, "Oxides, porosity and fatigue performance of AlSi10Mg parts produced by selective laser melting", International Journal of Fatigue xxx (2016) .94(2) (2017) 192-201
279. Ahmad Bin Anwar, Quang-Cuong Pham, "Selective Laser Melting of AlSi10Mg: Effects of scan direction, part placement and inert gas flowvelocity on tensile strength, *Journal of Materials Processing Tech.240 (2017) 388-396*
280. A. A Raus1, , M. S. Wahab , Z. Shayfull2 ,K. Kamarudin1 and M. Ibrahim, The Influence of Selective Laser Melting Parameters on Density and Mechanical Properties of AlSi10Mg, MATEC Web of Conferences .78(2016) 01078
281. K. Kamarudin, M. S. Wahab, A. A. Raus, Aqeel Ahmed, S. Shamsudin, Benchmarking of dimensional accuracy and surface roughness for AlSi10Mg part by selective laser melting (SLM), AIP Conf. Proc.1831 (2017) 020047
282. Lianfeng Wang, Xiaohui Jiang, Miaoxian Guo, Xiaogang Zhu & Biao Yan (2017): Characterisation of structural properties for AlSi10Mg alloys fabricated by selective laser melting, Materials Science and Technology, materials science and technology.33(18) (2017) 2274-2282
283. Aqeel Ahmed, M. S. Wahab, A. A. Raus, K. Kamarudin, Qadir Bakhsh and Danish Ali,Effects of Selective Laser Melting Parameters on Relative Density of AlSi10Mg, International Journal of Engineering and Technology (IJET).8(6) (2016) 2552-2557
284. J. Zou , Y. Zhua, M. Pan , T. Xie , X. Chen , H. Yang, A study on cavitation erosion behavior of AlSi10Mg fabricated by selective laser melting (SLM), Wear376-377(2017)496–506
285. Wang L-z, Wang S, Wu J-j (2017) Experimental investigation on densification behavior and surface roughness of AlSi10Mg powders produced by selective laser melting. Opt Laser Technol 96: 88–96
286. Naoki Takata, Hirohisa Kodaira1, Asuka Suzuki, Makoto Kobashi, Size dependence of microstructure of AlSi10Mg alloy fabricated by selective laser melting, Materials Characterization.143 (2018) 18-26
287. Awd M, Stern F, Kampmann A, Kotzem D, Tenkamp J, Walther F (2018) Microstructural Characterization of the Anisotropy and Cyclic Deformation Behavior of Selective Laser Melted AlSi10Mg Structures. Metals. 8(10):825

288. Biffi CA, Fiocchi J, Bassani P, Tuissi A (2018) Continuous wave vs pulsed wave laser emission in selective laser melting of AlSi10Mg parts with industrial optimized process parameters: microstructure and mechanical behaviour. *Additive Manufacturing* 24:639–646
289. Zhichao Dong , Xiaoyu Zhang , Wenhua Shi , Hao Zhou , HongshuaiLei,and Jun Liang, Study of Size Effect on Microstructure and Mechanical Properties of AlSi10Mg Samples Made by Selective Laser Melting, Materials **.11(12) (2018) 2463**
290. Mfusi BJ, Tshabalala LC, Popoola API, Mathe NR (2018) The effect of selective laser melting build orientation on the mechanical properties of AlSi10Mg parts. IOP Conf Series: Materials Science and Engineering **430**:012028
291. Song B, Yan Q, Shi Y (*2020*) Comparative study of performance comparison of AlSi10Mg alloy prepared by selective laser melting and casting. *J Mater Sci Technol 41:199–208*
292. Tianyu Yu , Holden Hyer, Yongho Sohn , Yuanli Bai , DazhongWu," Structure-property relationship in high strength and lightweight AlSi10Mg microlattices fabricated by selective laser melting Materials and Design 182 (2019) 108062
293. Zhong-hua Li, Yun-feiNie, Bin Liu, Ze-zhou Kuai, Miao Zhao,Fei Liu, Mechanical properties of AlSi10Mg lattice structures fabricated by selective laser melting, Materials & Design.192(2020) 108709
294. Dong Z, Liu Y, Li W, Liang J (2019) Orientation dependency for microstructure, geometric accuracy and mechanical properties of selective laser melting AlSi10Mg lattices. J Alloys Compd 791: 490–500
295. Chen B, Yao Y, Song X, Tan C, Liang C, Feng J (2018) Microstructure and mechanical properties of additive manufacturing AlSi10Mg alloy using direct metal deposition. Ferroelectrics 523:153–166
296. G. Struzikiewicz , W. Ze˛bala, B. Słodki, "Cutting parameters selection for sintered alloy AlSi10Mg longitudinal turning"Measurement 138 (2019) 39–53
297. Palumbo B, Del Re F, Martorelli M, Lanzotti A, Corrado P (2017) Tensile properties characterization of AlSi10Mg parts produced by direct metal laser sintering via nested effects modeling. Materials 10(2):144
298. Ghasri-Khouzania M, Peng H, Attardo R, Ostiguy P, Neidig J, Billo R, Hoelzle D, Shankar MR (2019) Comparing microstructure and hardness of direct metal laser sintered AlSi10Mg alloy between different planes. J Manuf Process 37:274–280
299. Calignano F, Manfredi D, Ambrosio EP, Iuliano L, Fino P (2013) Influence of process parameters on surface roughness of aluminum parts produced byDMLS. Int J Adv Manuf Technol 67: 2743–2751
300. BehroozJalalahmadi, Jingfu Liu, Jason Rios, John Slotwinski, ChristopherPeitsch, Arnold Goldberg, Timothy Montalbano,In-process defect monitoring and correction in additive manufacturing of aluminum alloys, Presented at the Vertical Flight Society's 75th Annual Forum & Technology Display, Philadelphia, PA, USA, May 13-16, 2019
301. F. Calignanoa,, G. Cattanob,, D. Manfredi,"Manufacturing of thin wall structures in AlSi10Mg alloy by laser powder bed fusion through process parameters",Journal of Materials Processing Tech. 255 (2018) 773–783
302. HitzlerE,Sert· E., Schuch A, Öchsner · M, Merkel3, B. Heine4 · E. Werner, Fracture toughness of L-PBF fabricated aluminium–silicon: a quantitative study on the role of crack growth direction with respect to layering, Progress in Additive Manufacturing . 5 (2020)259–266
303. Alexandra Inberg , Dana Ashkenazi ,Giora Kimmel · YosiShacham , Diamand, Adin Stern, Gold plating of AlSi10Mg parts produced by a laser powder-bed fusion additive manufacturing technique, Progress in Additive Manufacturing. . 5(2020) 395-404
304. N. Dresler, A. Inberg,D. Ashkenazi ,Y. Shacham-Diamand, · A. Stern, Silver Electro less Finishing of Selective Laser Melting 3D-Printed AlSi10Mg Artifacts, Metallography, Microstructure, and Analysis. 8(2019) 678-692
305. Scherillo F (2019) Chemical surface finishing of AlSi10Mg components made by additive Manufacturing. Manufacturing Letters 19:5–9
306. Xiaodong Xing , Xiaoming Duan , Tingting Jiang , Jiandong Wang and Fengchun Jiang, Ultrasonic Peening Treatment Used to Improve Stress Corrosion Resistance of AlSi10Mg Components Fabricated Using Selective Laser Melting, Metals .9(1) (2019) 103.
307. Maamoun AH, Elbestawi MA, Veldhuis SC (2018) Influence of Shot Peening on AlSi10Mg Parts Fabricated by Additive Manufacturing. J Manuf Mater Process 2(3):40
308. James Damon, Stefan Dietrich, Florian Vollert,JensGibmeier, Volker Schulze, Process dependent porosity and the influence of shot peening on porosity morphology regarding selective laser melted AlSi10Mg parts, Additive Manufacturing. 20 (2018) 458-464.
309. NE, Ramati S, Shneck R, Frage N, Yeheskel O, On the effect of shot-peening on fatigue resistance of AlSi10Mg specimens fabricated by additive manufacturing using selective laser melting (AM-SLM), Additive Manufacturing . 21 (2018) 458-464.
310. Author: E. Atzeni M. Barletta F. Calignano L. IulianoG. Rubino V. Tagliaferri, Abrasive Fluidized Bed (AFB) finishing of AlSi10Mg substrates manufactured by Direct Metal Laser Sintering (DMLS),Additive Manufacturing. 10 (2016) 15-23
311. Andrea El Hassanin, Maurizio Troiano, Alessia Teresa Silvestri, VincenzoContaldi, Fabio Scherillo, Roberto Solimene,Fabrizio Scala , Antonino Squillace and Piero Salatino, Influence of Abrasive Materials in Fluidised Bed Machining of AlSi10Mg Parts Made through Selective Laser Melting Technology,Key Engineering Materials. 183 (2019) 129-134.
312. Xiao Teng, Guixiang Zhang,Yugang Zhao & Yuntao Cui, Linguang Li & Linzhi Jiang, Study on magnetic abrasive finishing of AlSi10Mg alloy prepared by selective laser melting, The International Journal of Advanced Manufacturing Technology, 105 (2019) 2513-2521
313. U. Tradowsky, J. White, R.M. Ward, N. Read, W. Reimers, M.M. Attallah, Selective Laser Melting of AlSi10Mg: Influence of Post-Processing on the Microstructural and Tensile Properties Development.105 (2016) 212-222
314. Rosenthal RS, Stern A (2018) Heat treatment effect on the mechanical properties and fracture mechanism in AlSi10Mg fabricated by Additive Manufacturing Selective Laser Melting process. Materials Science & Engineering A 729:310–322
315. Hirata T, Kimura T, Nakamoto T (2020) Effects of hot isostatic pressing and internal porosity on the performance of selective laser melted AlSi10Mg alloys. Materials Science & Engineering A 772: 138713
316. Hastie JC, Kartal ME, Carter LN, Attallah MM, Mulvihill DM (2020) Classifying shape of internal pores within AlSi10Mg alloy manufactured by laser powder bed fusion using 3D X-ray micro computed tomography: Influence of processing parameters and heat treatment. Mater Charact 163:110225
317. Girelli L, Giovagnoli M, Tocci M, Pola A, Fortini A, Merlin M, La Vecchia GM (2019) Evaluation of the impact behaviour of AlSi10Mg alloy produced using laser additive manufacturing. Materials Science & Engineering A 748:38–51
318. Uzan NE, Shneck R, Yeheskel O, Frage N (2017) Fatigue of AlSi10Mg specimens fabricated by additive manufacturing selective laser melting (AM-SLM). Materials Science & Engineering A 704:229–237

319. Liu B, Li B-Q, Li Z (2019) Selective laser remelting of an additive layer manufacturing process on AlSi10Mg. Results in Physics 12: 982–988
320. Yu W, Sing SL, Chua CK, Tian X (2019) Influence of re-melting on surface roughness and porosity of AlSi10Mg parts fabricated by selective laser melting. J Alloys Compd 792:574–581
321. Wenhuiyu, Sweeleong sing, Xuelei tian, Chee kai chua, Effects of re-melting strategies on densification behavior and mechanical properties of selective laser melting AlSi10Mg parts, Proc. Of the 3rd Intl. Conf. on Progress in Additive Manufacturing,2010, pp.476-481.
322. Schanz J, Hofele M, Hitzler L, Merkel M, Riegel H (2016) Laser polishing of additive manufactured AlSi10Mg parts with an oscillating laser beam, machining, joining and modifications of advanced materials. Advanced Structured Materials 61:159–169
323. du Plessis A, Glaser D, Moller H, Mathe N, Tshabalala L, Mfusi B, Mostert R (2019) Pore closure effect of laser shock peening of additively manufactured AlSi10Mg. 3d Printing and Additive Manufacturing 6:245–252
324. Takata N, Liu M, Kodaira H, Suzuki A, Kobashi M (2020) Anomalous strengthening by supersaturated solid solutions of selectively laser melted Al–Si-based alloys. Additive Manufacturing 33:101152
325. Busisiwe J. Mfusi , Ntombizodwa R. Mathe , Lerato C. Tshabalala and Patricia AI. Popoola , The Effect of Stress Relief on the Mechanical and Fatigue Properties of Additively Manufactured AlSi10Mg Parts, Metals 9(11) (2016) 1216
326. Suzuki A, Sekizawa K, Liu M, Takata N, Kobashi M (2019) Effects of heat treatments on compressive deformation behaviors of lattice-structured alsi10mg alloy fabricated by selective laser melting. Adv Eng Mater:1900571
327. Hrbáčková T, Simson T, Koch J, Wolf G (2019) The effect of heat treatment on mechanical properties and microstructure of additively manufactured components. IOP Conf Series: Materials Science and Engineering 461:012026
328. Xiaohui Jiang , Wenjing Xiong, Lianfeng Wang, Miaoxian Guo and Zishan Ding, Heat treatment effects on microstructure-residual stress for selective laser melting AlSi10Mg,Materials science and Technology, 2019
329. Zakay A, Aghion E (2019) Effect of post-heat treatment on the corrosion behavior of alsi10mg alloy produced by additive manufacturing. The Minerals, Metals & Materials Society 71: 1150–1157
330. Tridello A, Fiocchi J, Biffi CA, Chiandussi G, Rossetto M, Tuissi A, Paolino DS (2019) VHCF response of Gaussian SLM AlSi10Mg specimens: Effect of a stress relief heat treatment. Int J Fatigue 124:435–443
331. EladUzan N, Shneck R, Yeheskel O, Frage N (2018) High- temperature mechanical properties of alsi10mg specimens fabricated by additive manufacturing using selective laser melting technologies (AM-SLM). Additive Manufacturing 24:257–263
332. Rubben T, Revilla RI, De Graeve I (2019) Influence of heat treatments on the corrosion mechanism of additive manufactured AlSi10Mg. Corros Sci 147:406–415
333. Zhuo L, Wang Z, Zhang H, Yin E, Wang Y, Xu T, Li C (2019) Effect of post-process heat treatment on microstructure and properties of selective laser melted AlSi10Mg alloy. Mater Lett 234: 196–200
334. Maamoun AH, Elbestawi M, Dosbaeva GK, Veldhuis SC (2018) Thermal post-processing of AlSi10Mg parts produced by Selective Laser Melting using recycled powder. Additive Manufacturing 21:234–247
335. Tang M, Pistorius PC (2017) Anisotropic mechanical behavior of AlSi10Mg parts produced by selective laser melting. The Minerals, Metals & Materials Society 69:516–522
336. Gong W, Qi J, Wang Z, Chen Y, Jiang J, Wang Z, Qi Y (2019) Microstructure and Mechanical Properties of Selective Laser Melting AlSi10Mg, 3rd International Symposium of Space Optical Instruments and Applications. Springer Proceedings in Physics 192:113–120
337. Li W, Li S, Liu J, Zhang A, Zhou Y, Wei Q, Yan C, Shi Y (2016) Effect of heat treatment on AlSi10Mg alloy fabricated by selective laser melting: Microstructure evolution, mechanical properties and fracture mechanism. Materials Science & Engineering A 663: 116–125
338. Fite J, Prameela SE, Slotwinski J, Weihs T (*2020*) Evolution of the microstructure and mechanical properties of additively manufactured AlSi10Mg during room temperature holds and low temperature aging. Additive Manufacturing *36:101429*
339. Majeed A, Ahmed A, Salam A, Sheikh MZ (2019) Surface quality improvement by parameters analysis, optimization and heat treatment of AlSi10Mg parts manufactured by SLM additive manufacturing. International Journal of Lightweight Materials and Manufacture 2(4):288–295
340. Majeed A, Muzamil M, Lv J, Liu B, Ahmad F (2019) Heat treatment influences densification and porosity of AlSi10Mg alloy thin-walled parts manufactured by selective laser melting technique. J Braz Soc Mech Sci Eng 41:267
341. Lv F, Shen L, Liang H, Xie D, Wang C, Tian Z (2019) Mechanical properties of AlSi10Mg alloy fabricated by laser melting deposition and improvements via heat treatment. Optik 179:8–18
342. Zhang, C., Zhu, H., Liao, H., Cheng, Y., Hu, Z., Zeng, X., Effect of heat treatments on fatigue property of selective laser melting AlSi10Mg, International Journal of Fatigue .116 (2018) 513-522.
343. Majeed A, Zhang YF, Lv JX, Peng T, Waqar S, Atta Z (2018) Study the effect of heat treatment on the relative density of slm built parts of alsi10mg alloy, CIE48 Proceedings. The University of Auckland, December 2-5
344. J. Fiocchi, .C.A. Biffi, C. Colombo, L.M. Vergani, and A. Tuissi, Ad Hoc heat treatments for selective laser melted Alsi10mg alloy aimed at stress-relieving and enhancing mechanical performances, Additive Manufacturing Validation and Control.72 (2020) 1118-1127
345. Di Giovanni MT, de Menezes JTO, Bolelli G, Cerri E, Castrodez EM (2019) Fatigue crack growth behavior of a selective laser melted AlSi10Mg. Eng Fract Mech 217:106564
346. Qiu L, Wang F, Yang Y, Guo L (2019) A new modification effect of eutectic Si in selective laser melted AlSi10Mg. Mater Sci Technol 35(6):709–715
347. DomfangNgnekou JN, Nadot Y, Henaff G, Nicolai J, Kan WH, Cairney JM, Ridosz L (2019) Fatigue properties of AlSi10Mg manufactured by Additive Layer Manufacturing. Int J Fatigue 119:160–172
348. Brandl E, Heckenberger U, Holzinger V, Buchbinder D (2012) Additive manufactured AlSi10Mg samples using Selective Laser Melting (SLM): Microstructure, high cycle fatigue, and fracture behavior. Mater Des 34:159–165
349. Iturrioz A, Gil E, Petite MM, Garciandia F, Mancisidor AM, Sebastian MS (2018) Selective laser melting of AlSi10Mg alloy: influence of heat treatment condition on mechanical properties and microstructure. International Institute of Welding 62:885–892
350. Zyguła K, Nosek B, Pasiowiec H, Szysiak N (2018) Mechanical properties and microstructure of AlSi10Mg alloy obtained by casting and SLM technique. WSN 104:462–472
351. Casati R, Nasab MH, Coduri M, Tirelli V, Vedani M (2018) Effects of platform pre-heating and thermal-treatment strategies on properties of AlSi10Mg alloy processed by selective laser melting. Metals 8(11):954
352. Fousová M, Dvorský D, Michalcová A, Vojtěch D (2018) Changes in the microstructure and mechanical properties of

additively manufactured AlSi10Mg alloy after exposure to elevated temperatures. Mater Charact 137:119–126
353. Aboulkhair NT, Maskery I, Tuck C, Ashcroft I, Everitt NM (2016) The microstructure and mechanical properties of selectively laser melted AlSi10Mg: The effect of a conventional T6-like heat treatment. Materials Science & Engineering A 667:139–146
354. Seabra M et al (2016) Selective laser melting (SLM) and topology optimization for lighter aerospace components. Procedia Struct Integr 1:289–296
355. Anil S, Anand PS, Alghamdi H, Jansen JA (2011) Dental implant surface enhancement and Osseo integration. In Tech Open Access Publ 1:83–108
356. Asgari H, Baxter C, Hosseinkhani K, Mohammadi M (2017) On microstructure and mechanical properties of additively manufactured AlSi10Mg_200C using recycled powder. Materials Science & Engineering A 707:148–158
357. Fathi P, Mohammadi M, Duan X, Nasiri AM (2018) A comparative study on corrosion and microstructure of direct metal laser sintered AlSi10Mg_200C and die cast A360.1 aluminum. Journal of Materials Processing Tech 259:1–14
358. Mohammadi M, HamedAsgari (2018) Achieving low surface roughness AlSi10Mg 200C parts using direct metal laser sintering. Additive Manufacturing 20:23–32
359. Fatemi A, Molaei R, Sharifimehr S, Phan N, Shamsaei N (2017) Multi axial fatigue behavior of wrought and additive manufactured Ti-6Al-4 V including surface finish effect. Int J Fatigue 100:347–366
360. Leon A, Aghion E (2017) Effect of surface roughness on corrosion fatigue performance of AlSi10Mg alloy produced by selective laser melting (SLM). Mater Charact 131:188–194
361. Alrbaey K, Wimpenny D, Tosi R, Manning W, Moroz A (2014) On optimization of surface roughness of selective laser melted stainless steel parts: a statistical study. J Mater Eng Perform 23: 2139–2148
362. Read N, Wang W, Essa K, Attallah MM (2015) Selective laser melting of AlSi10Mgalloy: process optimization and mechanical properties development. Mater.Des. 65:417–424
363. Bacchewar PB, Singhal SK, Pandey PM (2007) Statistical modelling and optimization of surface roughness in the selective laser sintering process. Proc Inst Mech Eng Part B: J Eng Manuf 221: 35–52
364. Polmear IJ (2006) Light alloys: from traditional alloys to nan crystals. Elsevier, Oxford, UK
365. Kimura T, Nakamoto T (2016) Microstructures and mechanical properties of A356 (AlSi7Mg0.3) aluminum alloy fabricated by selective laser melting. Materials Design 89:1294–1301
366. Heng Rao, Stephanie Giet , Kun Yang , Xinhua Wu, Chris H.J. Davies," The influence of processing parameters on aluminium alloy A357 manufactured by Selective Laser Melting, Materials and Design 109 (2016) 334–346
367. Aversa A, Lorusso M, Trevisan F, Ambrosio EP, Calignano F, Manfredi D, Biamino S, Fino P, Lombardi M, Pavese M (2017) Effect of process and post-process conditions on the mechanical properties of an A357 alloy produced via laser powder bed fusion. Metals 7(2):68
368. Yang KV, Rometsch P, Jarvis T, Rao J, Cao S, Davies C, Wu X (*2018*) Porosity formation mechanisms and fatigueresponse in Al-Si-Mg alloys made by selective laser melting. Materials Science & Engineering A *712:166–174*
369. Yang KV, Rometsch P, Davies CHJ, Huang A, Wu X (2018) Effect of heat treatment on the microstructure and anisotropy in mechanical properties of A357 alloy produced by selective laser melting. Mater Des 154:275–290
370. Bassoli E, Denti L, Comin A, Sol A, Togno E (2018) Fatigue behavior of as-built L-PBF A357.0 parts. Metals 8(8):634
371. Tonelli L, Liverani E, Valli G, Fortunato A, Ceschini L (2020) Effects of powders and process parameters on density and hardness of A357 aluminum alloy fabricated by selective laser melting. Int J Adv Manuf Technol 10(6):371–383
372. Rao JH, Zhang Y, Zhang K, Wu X, Huang A (2019) Selective laser melted Al-7Si-0.6Mg alloy with in-situ precipitation via platform heating for residual strain removal. Mater Des 182:108005
373. Lorusso M, Trevisan F, Calignano F, Lombardi M, Manfredi D (2020) A357 Alloy by LPBF for industry applications. Materials 13:1488
374. Li YX, Zhang PF, Bai PK, Wu LY, Liu B, Zhao ZY (2018) Microstructure and properties of Ti/TiBCN coating on 7075 aluminum alloy by laser cladding. Surf Coat Technol 334:142–149
375. Zhao X, Song B, Fan WR, Zhang YJ, Shi YS (2016) Selective laser melting of carbon/ AlSi10Mg composites: microstructure, mechanical and electronical properties. J Alloys Compd 665: 271–281
376. Laorden LM, Rodrigo P, Torres B, Rams J (2017) Modification of microstructure and superficial properties of A356 and A356/10%SiCp by selective laser surface melting (SLSM). Surf Coat Technol 309:1001–1009
377. Bao S, Tang K, Kvithyld A, Tangstad M, Engh TA (2011) Wettability of Aluminum on Alumina. Metall Mater Trans B Process Metall Mater Process Sci 42(6):1358–1366
378. Shen P, Fujii H, Matsumoto T, Nogi K (2004) Critical Factors Affecting the Wettability of a-Alumina by Molten Aluminum. J Am Ceram Soc 87(7):1265–1273
379. Sercombe TB, Schaffer GB Rapid manufacturing of aluminum components. Science 301(5637):1225–1227
380. Gu DD (2015) Laser additive manufacturing of high-performance materials, Springer-Verlag. Berlin 2015
381. Gu DD, Chang F, Dai DH (2015) Selective laser melting additive manufacturing of novel aluminum based composites with multiple reinforcing phases. ASME J Manuf Sci Eng 137(2):021010
382. Fu CH, Guo YB (2014) Three-Dimensional Temperature Gradient Mechanism in selective laser melting of Ti-6Al-4V. ASME J Manuf SciEng 136(6):061004
383. Yadroitsev I, Bertrand P, Smurov I (2007) Parametric analysis of the selective laser melting process. Appl Surf Sci 253:8064–8069
384. Jue JB, Gu DD, Chang K, Dai DH (2016) Microstructure evolution and mechanical properties of Al-Al2O3 composites fabricated by selective laser melting. Powder Technol 310:80–91
385. Olakanmi EO (2013) Selective laser sintering/melting (SLS/SLM) of pure Al, Al-Mg, and Al-Si powders: Effect of processing conditions and powder properties. J Mater Process Technol 213(8): 1387–1405
386. Gu DD, Ma CL, Xia MJ, Dai DH, Shi QM (2017) A multiscale understanding of the thermodynamic and kinetic mechanisms of laser additive manufacturing. Engineering 3:675–684
387. Dai DH, Gu DD (2016) Influence of thermodynamics within molten pool on migration and distribution state of reinforcement during selective laser melting of AlN/ AlSi10Mg composites. Int J Mach Tools Manuf 100:14–24
388. Song B, Wang ZW, Yan Q, Zhang YJ, Zhang JL, Cai C, Wei QS, Shi YS (2017) Integral method of preparation and fabrication of metal matrix composite: selective laser melting of in-situ nano/submicro-sized carbides reinforced iron matrix composites. Mater Sci Eng A 707:478–487
389. Almangour B, Grzesiak D, Yang JM (2017) Scanning strategies for texture and anisotropy tailoring during selective laser melting of TiC/316L stainless steel nanocomposites. J Alloys Compd 728: 424–435
390. Gu DD, Meng GB, Li C, Meiners W, Poprawe R (2012) Selective laser melting of TiC/Ti bulk nanocomposites: influence of nanoscale reinforcement. Scr Mater 67:185–188

391. Han QQ, Geng YQ, Setchi R, Lacan F, Gu DD, Evans SL (2017) Macro and nanoscale wear behaviour of Al-Al2O3 nanocomposites fabricated by selective laser melting. Compos Part B Eng 127: 26–35
392. Thijs L, Kempen K, Kruth J-P, Van Humbeeck J (2013) Fine-structured aluminium products with controllable texture by selective laser melting of pre-alloyed AlSi10Mg powder. Acta Mater 61:1809–1819
393. Aboulkhair NT, Tuck C, Ashcroft I, Maskery I, Everitt NM (2015) On the precipitation hardening of selective laser melted AlSi10Mg. Metall Mater Trans A 46:3337–3341
394. Leon A, Aghion E (2017) Effect of surface roughness on corrosion fatigue performance of AlSi10Mg alloy produced by Selective Laser Melting (SLM). Mater Charact 131:188–194
395. Dai D, Dongdong G (2016) Influence of thermodynamics within molten pool on migration and distribution state of reinforcement during selective laser melting of AlN/AlSi10Mg composites. Int J Mach Tool Manu 100:14–24
396. Daia D, Gua D, Xiaa M, Maa C, Chena H, Zhao T, Hong C, Gasser A, Poprawe R (2018) Melt spreading behavior, microstructure evolution and wear resistance of selective laser melting additive manufactured AlN/AlSi10Mg nanocomposite. Surf Coat Technol 349:279–288
397. Dai D, Gu D, Poprawe R, Xia M (2017) Influence of additive multilayer feature on thermodynamics, stress and microstructure development during laser 3D printing of aluminum-based material. Sci Bull 62:779–787
398. Dongdong G, Jue J, Dai D, Lin K, Chen W (2018) Effects of dry sliding conditions on wear properties of al-matrix composites produced by selective laser melting additive manufacturing. J Tribol 740:021605
399. Liao H, Zhu H, Xue G, Zeng X (2019) Alumina loss mechanism of Al_2O_3-AlSi10 Mg composites during selective laser melting. J Alloys Compd 785:286–295
400. Dadbakhsh S, Hao L (2012) Effect of Al alloys on selective laser melting behaviour and microstructure of in situ formed particle reinforced composites. J Alloys Compd 541:328–334
401. Lorusso M, Aversa A, Manfredi D, Calignano F, Ambrosio EP, Ugues D, Pavese M (2016) Tribological behavior of aluminum alloy AlSi10Mg-TiB2 composites produced by direct metal laser sintering (DMLS). Journal of Materials Engineering and Performance, ASM International 25:3152–3160
402. Li Y, Gu D, Zhang H, Xi L (2020) Efect of trace addition of ceramic on microstructure development and mechanical properties of selective laser melted AlSi10Mg alloy. Chin J Mech Eng 33:33
403. Li XP, Ji G, Chen Z, Addad A, Wu Y, Wang HW, Vleugels J, Van Humbeeck J, Kruth JP (2017) Selective laser melting of nano-TiB2 decorated AlSi10Mg alloy with high fracture strength and ductility. Acta Mater 129:183–193
404. Zhao Z, Bai P, Misra RDK, Li MDRGY, Zhang J, Tan L, Ding JGT, Du W, Guo Z (2019) AlSi10Mg alloy nanocomposites reinforced with aluminum-coated graphene: Selective laser melting, interfacial microstructure and property analysis. J Alloys Compd 792:203–214
405. Tiwari JK, Mandal A, Sathish N, Agrawal AK, Srivastava AK (2020) Investigation of porosity, microstructure and mechanical properties of additively manufactured graphene reinforced AlSi10Mg composite. Additive Manufacturing 33:101095
406. Wang Y, Shi J (2020) Effect of hot isostatic pressing on nanoparticles reinforced AlSi10Mg produced by selective laser melting. Materials Science & Engineering A 288:139570
407. Liu X, Zhao C, Zhou X, Eibl F, Shen Z, Liu W, Meiners W (2019) CNT-reinforced AlSi10Mg composite by selective laser melting: microstructural and mechanical properties. Mater Sci Technol: 1038–1045
408. Zhao X, Song B, Fan W, Zhang Y, Shi Y (2016) Selective laser melting of carbon/ AlSi10Mg composites: microstructure, mechanical and electronical properties. J Alloys Compd 665:271–281
409. C. Gaoa, , Z. Wanga , Z. Xiaoa, , D. Youa , K. Wongc , A.H. Akbarzadeh,Selective laser melting of TiN nanoparticle-reinforced AlSi10Mg composite: Microstructural, interfacial, and mechanical properties, Journal of Materials Processing Tech 281 (2020) 116618